

The copyright of this thesis vests in the author. No quotation from it or information derived from it is to be published without full acknowledgement of the source. The thesis is to be used for private study or non-commercial research purposes only.

Published by the University of Cape Town (UCT) in terms of the non-exclusive license granted to UCT by the author.



**STRUCTURAL AND COMPOSITIONAL STUDIES OF
POTENTIAL IMMUNOMODULATORY POLYSACCHARIDES
FOUND IN LOCALLY GROWN PLANTS**

RONICA RAMSOUT

**STRUCTURAL AND COMPOSITIONAL STUDIES OF
POTENTIAL IMMUNOMODULATORY
POLYSACCHARIDES FOUND IN LOCALLY GROWN
PLANTS**

Dissertation presented to the
UNIVERSITY OF CAPE TOWN

In fulfilment of the requirements for the degree of
MASTER OF SCIENCE

By

RONICA RAMSOUT

B Sc Hons

Supervisors: Assoc. Professor Neil Ravenscroft
Dr Elizabeth Timme

Department of Chemistry
University of Cape Town
2007

DECLARATION

I declare that STRUCTURAL AND COMPOSITIONAL STUDIES OF POTENTIAL IMMUNOMODULATORY POLYSACCHARIDES FOUND IN LOCALLY GROWN PLANTS is my own work and that all the sources that I have used or quoted have been indicated and acknowledged my means of complete references.

signature removed

Ronica Ramsout

University of Cape Town

CONTENTS

	PAGE
ABSTRACT	i
ACKNOWLEDGEMENTS	iii
ABBREVIATIONS	iv
INDEX TO FIGURES	vi
INDEX TO TABLES	viii
1. INTRODUCTION	1
1.1 Plant polysaccharides	1
1.2 The aloe species	4
1.2.1 <i>Aloe vera</i>	6
1.2.1.1 <i>Structure of the plant</i>	6
1.2.1.2 <i>The commercial importance of Aloe vera</i>	6
1.2.1.3 <i>An important glucomannan – acemannan</i>	7
1.2.2 <i>Aloe ferox</i>	9
1.2.2.1 <i>Structure of the plant</i>	9
1.2.2.2 <i>The commercial importance of Aloe ferox</i>	9
1.2.2.3 <i>Objectives</i>	10
1.3 The agave species	11
1.3.1 <i>Fructans</i>	11
1.3.2 <i>Inulin</i>	12
1.3.3 <i>Nutritional importance of prebiotics</i>	13
1.3.4 <i>Structure – function relation</i>	14
1.3.5 <i>Commercial importance</i>	15
1.3.6 <i>Agave americana</i>	16
1.3.7 <i>Objectives</i>	17
1.4 Economic factors	18
2. METHODS	19
2.1 Sugar analyses	19
2.1.1 <i>Colorimetric analysis</i>	19
2.1.2 <i>Composition analysis</i>	20
2.2 Methylation analysis	20
2.3 Size-exclusion chromatography	21
2.4 Analysis by gas chromatography	23

2.5 Analysis by high-performance anion-exchange chromatography	24
2.6 Nuclear magnetic resonance spectroscopy	26
3. ALOE FEROX	29
3.1 Processing of <i>Aloe ferox</i> raw material	29
3.2 Size and composition analysis of water-soluble epidermis extracts A and B	31
3.2.1 Size analysis of extracts A and B	31
3.2.2 Composition analysis of extracts A and B	33
3.3 Size and composition analysis of water-soluble epidermis extract C	35
3.3.1 Size analysis of extract C by SEC with carbohydrate and uronic acid assay	35
3.3.2 Composition analysis of extract C by HPAEC-PAD	37
3.4 Additional compositional studies	42
3.5 Size analysis of water extract of ultrasound treated <i>Aloe ferox</i> parenchyma	44
3.6 Comparative study of leaves from <i>Aloe ferox</i> trees growing under different environmental conditions	46
3.7 Conclusion	49
4. AGAVE AMERICANA	50
4.1 Preparation of water-soluble material	50
4.2 Size analysis	51
4.2.1 Size analysis by SEC	51
4.2.2 Size analysis by HPAEC-PAD	53
4.3 Composition analysis	55
4.3.1 Composition analysis by HPAEC-PAD	55
4.3.2 Linkage assignments by methylation analysis	55
4.4 Structure analysis by NMR Spectroscopy	62
4.5 Conclusion	70
5. CONCLUSION	72
REFERENCES	74
APPENDIX	80

ABSTRACT

This project looked at the composition and structure of polysaccharides extracted from two locally grown plants, namely *Aloe ferox* and *Agave americana*, to evaluate them as possible sources of commercial health products.

Aloe vera, a well known medicinal plant with many healing properties, contains acemannan, a highly water-soluble mannose rich glucomannan, which has demonstrated immunogenic responses in humans and animals. *Aloe ferox*, a locally grown species, is commercially marketed as an equivalent to *Aloe vera* and is being substituted in various health products. This project examined the suitability of *Aloe ferox* as a substitute for *Aloe vera* by investigating the chemical nature of the water-soluble *Aloe ferox* polysaccharides. Findings from composition analysis revealed that polysaccharides found in the leaves of *Aloe ferox* are not mannose rich and are not highly soluble in water, like their *Aloe vera* counterparts; but instead are more readily soluble in aqueous $(\text{NH}_4)_2\text{C}_2\text{O}_4$ as previously reported. Size analysis showed that the water-soluble polymeric material is mostly of low-molecular weight. These smaller molecules are thought to be pectic polymers. The results obtained suggest that *Aloe ferox* cannot be considered as a suitable immunomodulatory substitute for *Aloe vera*.

Agave americana is a locally grown species of agave used in alcoholic beverage production. However, this process consumes only the heart of the plant leaving a large quantity of leaf material as a by-product. The heart of the *Agave americana* plant is known to be rich in fructans which are storage polymers made up of fructose generally with a terminal glucose e.g. inulin. The monosaccharides in inulin are bonded via β -(2 \rightarrow 1) fructosyl-fructose glycosidic linkages. Inulin is well known for its prebiotic properties due to the β -configuration of the anomeric C2 which renders the polymer indigestible to the enzymes in the gastrointestinal tract. This project evaluates the potential of *Agave americana* as a commercial source of inulin by investigating three factors that determine the prebiotic potential of a carbohydrate polymer: molecular size, monosaccharide composition and the glycosidic linkages between the residues. Size analysis showed that water-soluble saccharides in *Agave americana* have an average degree of polymerisation of approximately 16. Composition analysis confirmed that the saccharides were composed of glucose and fructose. Methylation analysis and NMR studies revealed the saccharide contains a backbone of β -(2 \rightarrow 1) linked fructosyl-fructose units with a terminal 1-linked or an internal (1 \rightarrow 6) linked glucose residue. The polymer is branched via C6 of the fructose residues in the polysaccharide backbone to C2 of fructose residues. These results indicate that *Agave americana* has suitable prebiotic characteristics and could be a possible source of commercial inulin.

ACKNOWLEDGEMENTS

I would like to thank the following:

A/Prof Neil Ravenscroft whose passion for carbohydrate chemistry and enormous faith in NMR inspired the completion of this project,

Elizabeth Timme (CSIR) for her continued assistance and supervision of the project and proofreading the manuscript,

Priscilla Mensah and Meredith Hearshaw for being a wonderful office partners and for their friendship and advice during the project,

Sue Kinnes (UCT) and Paola Cescutti (Italy) for their input to methylation analysis,

Claire Lawrence, Marilyn Mentor and Malcolm McClean for the use of their lab facilities and equipment,

Klaus Achlietner for technical assistance and Dierdre Brooks special assistance,

Pete Roberts (UCT), Noel Hendriks (UCT) and Jean Mckenzie (SUN) for assistance in running NMR experiments,

The CSIR for financial assistance,

The BYS executive committee who always demonstrate the brighter side of varsity life and for all the fun, laughter and lunch meetings over the years,

My family, my buddies Sandra, Sami, and Tamalini, and Shah Naidoo for their constant care, love and spiritual encouragement,

And to my most dear friends HH KKS (Amsterdam) and SS NMC (Cape Town).

ABBREVIATIONS

~	approximately
AIR	alcohol insoluble residues
Ara	arabinose
cm	centimetre
°C	degree Celsius
CD	conductivity
Da	daltons
DP	degree of polymerisation
FID	flame ionisation detection
GC	gas chromatography
g	gram
Gal	galactose
Glc	glucose
f	furanose
Fru	fructose
h	hour(s)
HPAEC	high performance anion exchange chromatography
HPLC	high performance liquid chromatography
i.d.	internal diameter
kDa	kilodaltons
kHz	kilohertz
l	litres
M	molar
Man	Mannose
m/e	ratio of mass to electron charge
mg	milligrams
mL	milliliter
min	minute(s)
mM	millimolar
MMD	molecular mass distribution
MS	mass spectrometry
Mol	mole
MW	molecular-weight
µm	micrometer

n.d.	not determined
nm	nanometer
NMR	nuclear magnetic resonance
O	oxygen
<i>p</i>	pyranose
PAD	pulsed amperometric detection
PMAA	permethylated alditol acetate
ppm	parts per million
Rha	rhamnose
SEC	size exclusion chromatography
TFA	trifluoroacetic acid
v/v	volume per volume
w/w	weight per weight
Xyl	xylose

INDEX TO FIGURES

CHAPTER 1

1.1 Structure of a matrix polysaccharide with a polygalacturonic acid backbone	1
1.2 Framework of a xyloglycan; a fibrous polysaccharide	2
1.3 <i>Aloe ferox</i> leaf showing the epidermis, parenchyma and mucilaginous gel	5
1.4 The <i>Aloe vera</i> plant	6
1.5 Structure of a glucomannan backbone found in acemannan	7
1.6 The <i>Aloe ferox</i> plant	9
1.7 Structure of inulin	12
1.8 <i>Agave americana</i> plant	17

CHAPTER 2

2.1 Calibration of column 1 (Sephacryl S-400-HR)	22
2.2 Chromatogram of standards on <i>Carbopac</i> PA20 column	25

CHAPTER 3

3.1 Flow diagram of experimental procedure followed	29
3.2 Molecular mass distribution of saccharides in extract A	31
3.3 Molecular mass distribution of saccharides in extract B	32
3.4 Monosaccharide percentage composition in extracts A and B after hydrolysis (2 h)	33
3.5 Monosaccharide percentage composition in extracts A and B after hydrolysis (4 h)	33
3.6 Molecular mass distribution of saccharides in extract C	35
3.7 Comparison of phenol-sulphuric and carbazole assays of extract C	37
3.8 Monosaccharide percentage composition in extract C after a 2 h hydrolysis period	39
3.9 Monosaccharide percentage composition in extract C after a 4 h hydrolysis period	39
3.10 Monosaccharide percentage composition in extract C after an 8 h hydrolysis period	39
3.11 Monosaccharide percentage composition in extract C after different hydrolysis periods	40
3.12 Comparison of phenol-sulphuric and carbazole assays of water-soluble <i>Aloe ferox</i> parenchyma treated with ultrasound	44

3.13 Monosaccharide percentage composition of the two different extracts of the Riverside leaves	47
3.14 Monosaccharide percentage composition of the two different extracts of the CSIR leaves	47

CHAPTER 4

4.1 Molecular mass distribution of polymers in the water extract of <i>Agave americana</i> eluted on column 2 (Sephacryl S-100-HR)	51
4.2 Molecular mass distribution of polymers in the water extract of <i>Agave americana</i> eluted on column 3 (Biogel P2)	52
4.3 DP profiling of chicory inulin (Sigma standard) by HPAEC-PAD	54
4.4 DP profiling of <i>Agave americana</i> extract by HPAEC-PAD	54
4.5 Composition analysis of <i>Agave americana</i> saccharides by HPAEC-PAD	55
4.6 Structure of chicory inulin	56
4.7 Gas chromatography of permethylated alditol acetate derivatives of chicory inulin	56
4.8 Mass fragmentation pattern of peak a	57
4.9 Mass fragmentation pattern of peak b	57
4.10 Mass fragmentation pattern of peak c	58
4.11 Gas chromatography of permethylated alditol acetate derivatives of <i>Agave americana</i> water extract	59
4.12 Mass fragmentation pattern of peak e	60
4.13 Mass fragmentation pattern of peak d	61
4.14 Structure of saccharides in <i>Agave americana</i>	61
4.15 ¹ H NMR spectrum of chicory inulin	63
4.16 ¹³ C NMR spectrum of chicory inulin	63
4.17 The HSQC spectrum of chicory inulin	65
4.18 ¹ H NMR spectrum of the <i>Agave americana</i> water extract	66
4.19 ¹³ C NMR spectrum of the <i>Agave americana</i> water extract	67
4.20 The HSQC spectrum of the <i>Agave americana</i> water extract	68

INDEX TO TABLES

CHAPTER 3

3.1 Carbohydrate composition of <i>Aloe ferox</i> leaves	42
3.2 Monosaccharide percentage composition in the two different extracts of the two batches of leaves	46

CHAPTER 4

4.1 ^{13}C NMR chemical shifts in ppm of the β -D-Fruf and α -D-Glcp units of chicory inulin (Sigma standard)	64
--	----

University of Cape Town

1 Introduction

1.1 Plant polysaccharides

Polysaccharides in plants display versatile functionality as storage agents, protective substances and structural components. As storage agents, starch and glycogen are better known but there are other polysaccharide reserves e.g. glucans, fructans and galactomannans.^{1,2} Protective polysaccharides in plants function as antigenic and immunogenic agents towards microorganisms. They are usually gums that serve as physical barriers over injured parts of plants.²

Structural polysaccharides fall into two distinct classes namely matrix and fibrous polysaccharides. Matrix polysaccharides have an inherent gel-forming capacity, which imparts flexibility to the structure. These are complex carbohydrates which comprise several different neutral and acidic polysaccharides, but are mainly a backbone of α -(1 \rightarrow 4) linked D-galacturonic acid units (Figure 1.1), with short side-chains of galactose, arabinose or rhamnose residues. Pectin is an example of such a matrix polysaccharide.^{1,2}

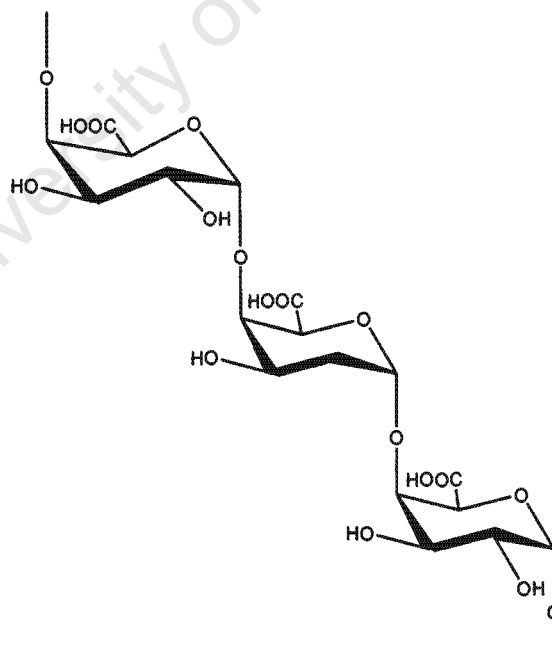


Figure 1.1: Structure of a matrix polysaccharide with a polygalacturonic acid backbone

Fibrous polysaccharides are commonly cellulosic but sometimes contain xylose polysaccharides (Figure 1.2); mannans in higher plants and algae; and chitin in yeast cells. In contrast to matrix polysaccharides, these molecules adopt regular chair conformations, which enable them to provide some rigidity to plant structures.¹

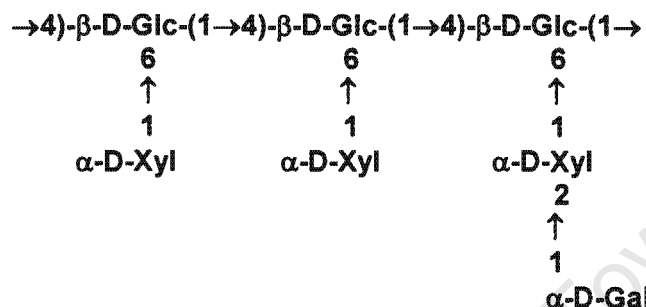


Figure 1.2: Framework of a xyloglycan; a fibrous polysaccharide

Polysaccharides found in plants have demonstrated many useful functions in the food industry and in the manufacture of health products. Insoluble cellulosic material derived from different botanical origins is used in the paper, fuel, lumber and textile industry. Cellulose is also fibrous in nature and is utilised as a source of dietary fibre.¹ Pectins are abundant polysaccharides commonly found in citrus fruit. Under certain conditions, pectins form gels. This property has made pectins an important additive in the confectionery industry.³

Polysaccharides derived from plant sources have demonstrated many immunomodulatory effects on humans. Glucomannans from *Aloe vera* have shown a positive effect in boosting the immune system by strengthening the body's own resistance to germs.⁴ Inulin, derived from plant sources has shown to act as a prebiotic.⁵ Prebiotics selectively stimulate the growth of beneficial bacteria in the colon and inhibit the growth of pathogenic bacteria thereby promoting good health.

The present study investigates the water-soluble polysaccharides isolated from a local species of aloe (*Aloe ferox*) and agave (*Agave americana*) as potential sources of medically beneficial polysaccharides suitable for commercial exploitation.

University of Cape Town

1.2 The aloe species

The ancient Egyptians described the aloe as the *Plant of Immortality* as it can live and even bloom without soil. The medicinal uses of aloe have been exploited since the first century and continue to be used today. The aloe genus contains at least 324 species which grow naturally throughout the tropics. However most are indigenous to Africa.⁶ The plant is quite widely found in southern Africa, in a broad range of habitats e.g. southern Kwazulu-Natal, Western Cape, the grassy fynbos in the Eastern Cape, the karoo as well as the south eastern Free State and Lesotho.

Of the 324 species of aloe known, most are non-toxic but there are a few that are extremely poisonous. Only 5 of these 324 species have demonstrated medical benefits, namely: *Aloe Barbadenis* Miller, *Aloe ferox*, *Aloe Perryi* Baker, *Aloe arborescens* and *Aloe saponaria*.⁷ *Aloe Barbadenis* Miller, more commonly known as *Aloe vera*, is the most widely grown species of aloe and considered to be the most potent with respect to its well known medicinal and therapeutic properties. To date it is the species of aloe that the most work has been carried out on. However, in the Eastern Cape there are two species of aloe, *Aloe ferox* and *Aloe arborescens* that grow abundantly and are targets for commercial exploitation.

The different species of aloe plants are quite similar in structure and usually reach maturity in about 4 years. They are xerophytes and grow well in dry arid conditions. However even though the plants are structurally similar, they do vary substantially in size.⁷ The leaves of the plant are of special importance as they contain the compounds of interest (Figure 1.3).

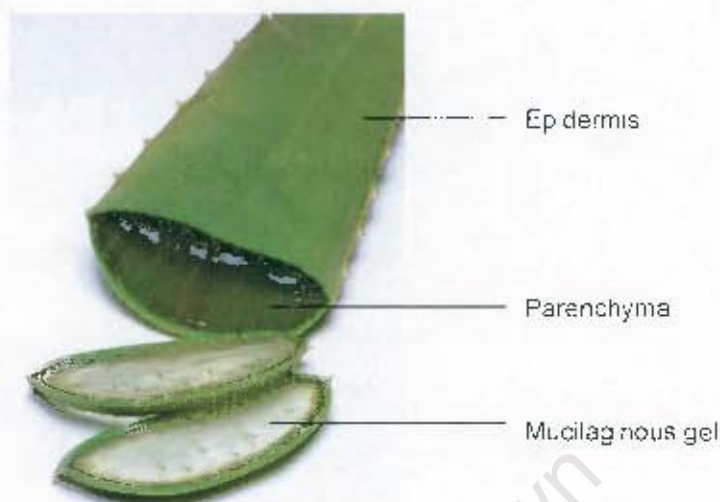


Figure 1.3: *Aloe ferox* leaf showing the epidermis, parenchyma and mucilaginous gel⁶

The epidermis (outer layer) has a thick protective cuticle. Underneath the epidermis is the mesophyll layer which contains the chlorenchyma and parenchyma cells. Parenchyma tissue comprises thin-walled cells which store a mucilaginous jelly-like substance which has been the target of research over the years.³⁻¹⁰

Quantitatively, apart from water (which makes up 99% of the plant), the largest component of aloe leaves are carbohydrates, consisting of some monosaccharides but mainly complex polymers. Other components present in aloe plants are amino acids, minerals, enzymes, lipids and acids.⁶⁻⁹

The complex polysaccharides present in aloe exist in various forms: pectins, mucopolysaccharides, glycoproteins and glucomannans, and account for their moisture holding properties. Previous studies on aloe glycoproteins show a high percentage of linear structures of glucose and mannose as well as linear linked glucans, branched arabinogalactans and linear mannans.¹¹

1.2.1 *Aloe vera*

1.2.1.1 *The structure of the plant*

Aloe vera (Figure 1.4), is a 'shrub-like' plant. Younger leaves grow at the base and old leaves taper towards the middle. The stem can grow up to 25 cm with 12-16 leaves per plant and at maturity the leaves can grow to a height of 60-90 cm and 5-10 cm across the base.⁷



Figure 1.4: The *Aloe vera* plant¹²

1.2.1.2 *The commercial importance of Aloe vera*

Aloe gel is derived from the parenchyma of the leaf of the *Aloe vera* plant. Commercially sold gel is a concentrated extract of the whole aloe leaf and is commonly used as an additive in the cosmetic industry.⁷ Its moisture transporting properties bring about nourishment and healing to dehydrated and damaged skin cells and it therefore acts as both a first-aid and beauty treatment.

1.2.1.3 An important glucomannan – acemannan

The main bioactive polysaccharide found in *Aloe vera* is acemannan, a glucomannan. It is commercially sold as Acemannan ImmunostimulantTM and Acemannan HydrogelTM also known as *Carrysin*. Acemannan ImmunostimulantTM has been successfully used in the treatment of fibrosarcoma of domestic animals, especially cats and dogs, and found to increase the activity of macrophages in humans. Acemannan HydrogelTM has been used in wound dressing for the treatment of cuts and abrasions.^{3,14 15}

The acemannan polysaccharide, which is highly water soluble, was found to contain 90 % carbohydrate, 1-2 % protein, less than 1 % insoluble matter and some organic salts. The polysaccharide exists as a polymer of various lengths due to differences in plant sub-species or different geographical origins.⁹ The polymer is highly mannose rich with a content of ~ 94 %.

There has been some uncertainty over the structure of the acemannan in literature, but the most recent work has revealed the following: acemannan has an O-acetylated, glucomannan backbone with an average molecular weight of approximately 2000 kDa.¹³ (Figure 1.5) The mannose to glucose residues exist in a ratio of 15:1. Branching on the polymer occurs from O2, O3 and O6 of 1,4 linked β -Manp residues in the polymer backbone with substitution by single α -Galp side chains.⁴

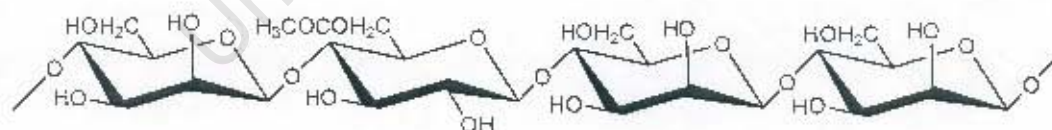


Figure 1.5: Structure of a portion of the glucomannan backbone found in acemannan

This purified polysaccharide has shown immunostimulatory properties by acting as an adjuvant on specific antibody production resulting in the enhanced release of cytokines: interleukin-1 (IL-1), interleukin-6 (IL-6), tumour necrosis factor- α (TNF- α) and

Initially, acemannan with its therapeutic properties was reported as a 3-(1,7)-acetylated mannan polymer of molecular size 80 kDa. Thereafter a 1000 kDa injectable form of acemannan was developed. Recently, another form of high-molecular weight polysaccharide was isolated (4000 – 7000 kDa) which showed even more effective immunostimulatory activity. In contrast a much smaller form of highly acetylated polysaccharide was isolated from aloe gel by cellulase treatment (80 kDa) and was reported to have much stronger immunomodulatory activity than the larger polysaccharides. However, the polysaccharides exhibiting the most potent immunomodulatory activity were found to have a molecular weight of between 0.4 – 5 kDa.¹⁹

Although there is common agreement on the relationships between size and function on the various immunomodulatory functions of the polysaccharides found in aloe gel, the optimal molecular size exhibiting immunomodulatory activity has not yet been established.

The release of these cytokines stimulates an increase in the replication of fibroblasts in tissue culture and enhances macrophage phagocytosis by up to 300 %. Fibroblasts are responsible for healing burns, ulcers, and other wounds of the skin and gastrointestinal lining. Acemannan has also been shown to inhibit AIDS virus replication *in vitro*, and an injectable form has found to be of significant benefit in FIV-infected cats.²⁰

1.2.2 *Aloe ferox*

1.2.2.1 Structure of the plant

Aloe ferox is a tall, single stemmed plant, with leaves arranged in a rosette (Figure 1.6). Dry, older leaves are found on the lower portion of the stem while fresh, younger leaves occur on the upper portion. The broad fleshy leaves are dull green in colour, with reddish to dark brown spines on the edges and sometimes on the lower surface. The plant can grow up to 3 meters tall and has bright red to orange flowers, which are arranged in a cluster at the tip of the plant.⁶



Figure 1.6: The *Aloe ferox* plant¹⁶

1.2.2.2 The commercial importance of *Aloe ferox*

Aloe ferox is commonly known as 'the bitter aloe', in reference to the bitter yellow, aloin rich juice that exudes from the vascular tissue just below the surface of the epidermis. The aloe bitters are mainly used as laxatives.¹⁷ Locally grown *Aloe ferox* is now being used as a source of aloe gels in products manufactured in South Africa.¹⁷ This is one of the three useable parts of aloe leaves – the other two being the green epidermis as a source of fibre and the white parenchyma which contains minerals, vitamins, amino acids, polysaccharides, enzymes and lipids.¹⁸ Not only have the 20 classical amino acids, usually found in proteins been found in *Aloe ferox*, but total of 37 different amino acids have been identified.¹¹

1.2.3 Objectives

Many years of research have gone into explaining the basis upon which aloe products display their remarkable and diverse properties. Findings so far have suggested that these properties may be due to the complex chemistry of the aloe plant.⁷ The chemistry of natural products has not only formed a scientific basis for the use of traditional medicinal plants, but has also motivated the discovery of many pharmaceutical and cosmetic bioactive ingredients.

The main objective of the present investigation was to determine the composition of the structural and functional polysaccharides found in the leaves of *Aloe ferox* plants that are easily extracted by water. These water-soluble polysaccharides will be analysed in an attempt to identify a glucomannan with similar physical and chemical properties to acemannan and if such a molecule is present, to consider the possibility of locally grown *Aloe ferox* as a viable substitute for *Aloe vera* in health products.

1.3 The agave species

Agaves are succulent plants of a large genus of the same name, belonging to the family *Agavaceae*. Although agaves can be found in the southern and western United States and in central and tropical South America, Mexico has been considered the centre of agave diversity. Of the species 310 known species, 272 are grown in Mexico.¹⁹ Due to the similar climatic conditions in South Africa and Mexico, the plant also grows abundantly in this country. Since the beginning of time, the various species of agave have been renowned for their use in the production of alcoholic beverages, especially tequila which is obtained by cooking the heart of the *Agave tequilana* plant.²⁰

Species of the *Agavaceae* family have adapted to growing in arid and semi-arid regions. This is possibly due to the plants undergoing some morphological and physiological changes in order to survive these adverse conditions. One of the physiological adaptations of the plant is the utilization of crassulacean acid metabolism (CAM) – a mechanism whereby the plants fix atmospheric CO₂ at night when temperatures are cooler.^{19,20} The opening of the stomata during the night decreases the transpirational loss of water from the plant to the environment.

The chief photosynthetic product of CAM in agave plants was found to be a fructan – a water-soluble fructose polymer generally with one terminal glucose residue.¹⁹

1.3.1 Fructans

In more developed plants, starch and sucrose are the most commonly known reserve carbohydrates. However, in almost 15 % of flowering plants, fructans have been found to carry out this function. Although the primary purpose of these fructans is to act as storage carbohydrates, they sometimes may also act as osmoprotectants.^{19,20} Fructans are naturally occurring storage polysaccharides made up of a family of oligo- and polysaccharides of fructose units, often with a terminal glucose molecule present. In higher plants, five structurally different types of fructans have been classified based on the nature of the glycosidic linkage present, namely: inulin, levan, mixed levan, inulin neoseris and levan neoseris.^{20,21}

1.3.2 Inulin

Inulin refers to a heterogeneous mix of fructose (F) polymers generally bearing a terminal glucose (G) unit. Inulin type fructans are fructose polymers with almost entirely β -(2 \rightarrow 1) fructosyl-fructose linkages, whereas levan-type fructans have mostly β -(2 \rightarrow 6) fructosyl-fructose linkages (Figure 1.7). Both types of fructans exist mostly as linear molecules, however a low degree of branching can exist. In the case of inulin, branching occurs via β -(2 \rightarrow 6) linkages and in levans through the β -(2 \rightarrow 1) bonds. In fructans, where the terminal glucose is absent, the terms inulo-*n*-oses and levan-*n*-oses are used.^{4,20-24}

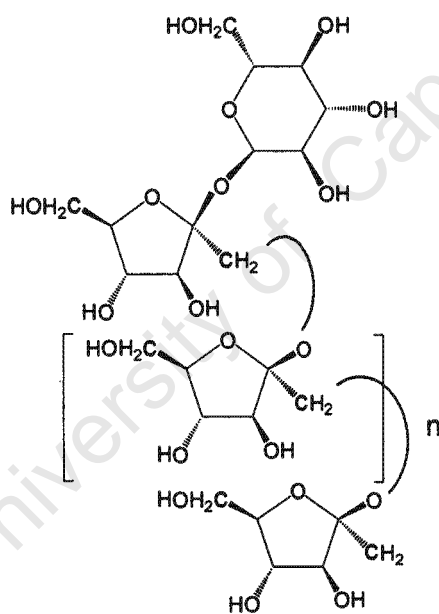


Figure 1.7: Structure of inulin

The molecular structure of inulin type fructans is usually referred to as GF_{*n*} (*n* = 3 to ~ 60). Fructooligosaccharides (FOS) or oligofructose refer to low-molecular weight fractions of inulin (*n* = 2 – 9).⁵ The unique feature of the inulin structure is its β -configuration of the anomeric C2 which prevents it from being digested like other typical carbohydrates.²² The enzyme fructanase, which is required for the hydrolysis of β -(2 \rightarrow 1)

linkages, is not present in the human digestive system therefore fructans are considered to be non-digestible.^{5,23,25}

To date, inulin is the most well known and studied fructan. It is found in more than 36 000 plant species but most prominently in wheat, onion, bananas, garlic and chicory.⁴ Fructans have proven to be of commercial importance as they have a wide range of applications in different industries, especially the food industry. Longer chain inulin polymers have been used as a fibre-type prebiotic with a number of health benefits. In recent years, dietary modulation of the human intestinal flora has been an area of focus, as an optimal gut microflora has been shown to be of immense benefit to health.²²

1.3.3 Nutritional importance – prebiotics

Prebiotics are food ingredients that selectively stimulate the growth of bacteria in the colon. Biological functions of the human colon include waste storage and elimination, as well as the absorption of mineral substances and water. The environment of the colon, the almost neutral pH and high substrate availability, makes it home to a very complex and diverse bacterial microflora. The microflora in the human large intestine, comprises almost 95 % of the total cells in the body, hence an active area of host nutrition and welfare.²⁶

The microflora composition in the gastrointestinal tract is a key factor for nutrition and health of the host. Over the years, the concept of functional food has evolved to where improvement of the gut microbial content has been the motivation towards the development of new food products.²⁶

Certain intestinal microbes are pathogenic and may be involved in the onset of some acute and chronic ailments, e.g. carcinogen production, intestinal putrefaction, toxin production and liver damage. However, some species are health promoting, e.g. bifidobacteria and lactobacilli. Some health benefits of lactobacilli include aiding lactose digestion in lactose intolerant individuals, reducing constipation and infantile diarrhoea, and helping to prevent salmonella infections. Bifidobacteria assist in strengthening the immune system, producing B vitamins, inhibiting pathogen growth, reducing blood ammonia and cholesterol levels, and helps to restore the normal microflora after

antibiotic treatment. The selective enhancements of growth of these beneficial bacterial species are therefore common targets for dietary modulation to improve an individual's health.^{5,26}

There are at least three criteria for a food product to be classified as a prebiotic: (1) the substrate must not be hydrolysed or absorbed in the stomach or small intestine, (2) it must be selective for the commensal and beneficial bacteria in the colon that are of benefit, (3) fermentation of the product should induce beneficial systematic effects within the host. The fundamental principle behind prebiotics is to induce certain indigenous intestinal bacteria rather than introducing exogenous species as is the case of probiotics. Promoting a dominating healthier gut micro-environment by prebiotics helps inhibit potential pathogenic toxin producing bacterial species.²⁶

Apart from modifying food products, prebiotics can be taken naturally through diet. Many fruit and vegetables, e.g. onion, garlic, banana, asparagus, leek, Jerusalem artichoke and chicory, contain prebiotic oligosaccharides such as FOS. However, the FOS content in these foods are probably too low to exert any significant effect. Some studies have indicated that between 4-8 g/day of FOS is needed to elevate bifidobacterium population considerably, hence the need to fortify food products with prebiotics.^{5,26}

1.3.4 Structure – function relation

The prebiotic potential of carbohydrates is mostly determined by the following factors: monosaccharide composition, glycosidic linkage and molecular weight.²⁶

The most abundant prebiotics are composed primarily of glucose, galactose, xylose and fructose. The glycosidic linkages between the monosaccharide residues are an essential factor in determining selectivity of fermentation and digestibility of the prebiotic. Degradation and utilization of FOS prebiotics by bifidobacteria is possible due to bifidobacteria possessing the enzyme β -fructofuranoside, which is not present in other bacterial species.²⁶

The difference in chain length between inulin and other FOS account for the difference in functional attributes. Compared with other prebiotic polysaccharides, inulin has the

highest molecular weight. The degree of polymerization (DP) of inulin can range from 11-60, depending on the grade of the product. Some food products contain inulin with an average DP of 14 whereas others with an average DP of 25.⁵

It is thought that the greater the polymer chain length, the greater the prebiotic effect exhibited, as a longer chain means that the fermentation process is slower, and the prebiotic effect will penetrate more effectively throughout the colon.²⁶

1.3.5 Commercial importance

Studies have indicated that all inulin and FOS consumed passed through the mouth, stomach and small intestine without being digested, and reached the colon where they are totally fermented by colonic bacteria, hence their application as a prebiotic. The energy derived from bacterial metabolism is largely due to the production of short-chain fatty acids and lactate.^{5,26}

FOS possess functional properties similar to those of sucrose or glucose syrup. Inulin with a low degree of polymerisation has been used as a low calorie sweetener as fructose is 1.6 times sweeter than glucose. Inulin and FOS have lower caloric value than typical carbohydrates due to the β -(2 \rightarrow 1) bonds between the fructose residues.⁵

The nondigestibility of inulin and FOS renders it suitable for consumption by diabetics. No changes in serum glucose, or stimulation of insulin and glucagon secretion were detected during research studies.⁵ Both inulin and FOS have also been successfully used to incorporate fibre into food products.

The longer chain length of inulin decreases its solubility enabling it to form inulin microcrystals when in water or milk. These crystals form a creamy texture and fat-like mouth-feel, allowing inulin to be successfully used as a fat substitute in baked goods, dairy products and desserts.⁵

Inulin has some non-food applications such as washing softener or biologically degradable plastics. Apart from the industrial applications of fructans, there has been some interest as a possible application in transgenic plant research. Fructan

accumulation has shown to give a higher dry weight in the aerial parts of plants. It is believed that this might impart drought tolerance or cold resistance.²¹

1.3.6 *Agave americana*

In the agave species more than one fructan type has been reported. In *Agave tequilana* and *Agave americana* species, the principal storage carbohydrate reported is an inulin polysaccharide with β -(2→1) linkages. In the *Agave vera cruz* species, a complex mixture of branched fructans was reported, with internal glucose moieties together with β -(2→1) and β -(2→6) fructosyl linkages. Recent studies on *Agave deserti* revealed a neokestose, a class of fructans (DP 3) with an internally linked glucose residue.¹⁹

Many species within the agave genus have been used to make different alcoholic beverages but *Agave tequilana* has been the species of choice cultivated for the production of tequila.²⁰

For the production of tequila, the heart of the plant, which constitutes 54 % of the wet plant, serves as raw material. The polymers present in hearts of the plants, mainly inulin, are hydrolysed into fermentable sugars. After harvesting the hearts for tequila production, the leaves of the plant are left out in the field to dry. These by-products (agave leaf fibres) have been utilized in a hand-pulping process to manufacture paper. These paper sheets had a breaking strength comparable with paper made from pine and eucalyptus fibres, and have the potential to be used in making paper products.²⁷

During the tequila making process, the agave hearts are cooked, thereafter shredded, milled and the sugars are extracted with water. The residual fibre remaining after this procedure is called bagasse. The bagasse is basically the rind and fibrous vascular tissue found in the interior of the agave heart. This by-product has been previously used for manufacturing mattresses, furniture and packing materials. More recently, agave bagasse has been utilised as a ruminant feed for livestock due to its function as a source of energy. When substituted for corn stubble in the sheep's diet, it resulted in the sheep gaining weight.²⁷

Another popular species of agave is *Agave americana* (Figure 1.8), a native of tropical America, sometimes known as the *Century Plant* or *American Aloe* (although not closely related to the genus *aloe*). The name *Century Plant* is in reference to the long time taken for the plant to flower.



Figure 1.8: *Agave americana* plant²⁸

1.3.7 Objectives

Agave americana is locally grown in South Africa, and the heart of the plant is used in the production of tequila. However in the process of tequila production, a large quantity of plant material i.e. the leaves remain as by-products. As part of a larger project on agro-reprocessing, both the heart and leaves of *Agave americana* are being evaluated as potential sources of commercial inulin. This project aims at characterising the composition and structure of the fructose rich saccharides produced by *Agave americana* by studying those isolated from in the heart.

1.4 Economic factors

This project looks at the viability of locally grown *Aloe ferox* and *Agave americana* as potential alternative raw materials in the production of different health products. *Aloe ferox* is being considered a substitute for the imported *Aloe vera* and *Agave americana* as source of commercial inulin.

The successful utilisation of *Aloe ferox* and *Agave americana* in commercial products will not only assist the *Proudly South African* brand campaign, whose emphasis is on producing lower cost South African equivalents to boost economic transformation and job growth, but will also accord with the current emphasis on *Green chemistry* with the utilisation of waste products.

2 Methods

In order to determine the composition and structure of polysaccharides present in the different extracts of *Aloe ferox* and *Agave americana*, various methods of analysis were employed.

Size-exclusion chromatography (SEC), coupled with colorimetric assays was used to screen the molecular weights of neutral and acidic polymers present in the different extracts. The composition of neutral sugars was analysed after hydrolysis by the use of high-performance anion-exchange chromatography with pulsed amperometric detection (HPAEC-PAD). Acidic monosaccharides were detected by high-performance anion-exchange chromatography with conductivity detection (HPAEC-CD).

Linkage composition was determined by methylation analysis of partially methylated alditol acetate derivatives (PMAA) of neutral monosaccharides using gas chromatography with flame ionisation detection (GC-FID). Gas chromatography coupled with mass spectrometry (GC-MS), was used to confirm the identity of the PMAA. Nuclear magnetic resonance (NMR), spectroscopy was used to investigate structural features of the oligo- and polysaccharides.

2.1 Sugar analyses

2.1.1. Colorimetric analysis

Colorimetric assays were used to quantify the neutral and charged saccharides. Neutral polysaccharides were identified by a phenol-sulphuric acid assay. In this reaction, the highly concentrated sulphuric acid depolymerises and dehydrates the sugar polymers which then complex with phenol to generate chromophores. The maximum absorption of these chromophores occurs at 490 nm.

A carbazole reaction was used to monitor acidic polysaccharides. The methodology of the colour reactions of the neutral and charged polysaccharides are given in Appendix 1.1 and 1.2 respectively.^{29,30}

2.1.2 Composition analysis

In order to determine the composition of saccharides in the extracts of *Aloe ferox* and *Agave americana*, the saccharides were first acid hydrolysed into monomers and the monosaccharides were identified by GC and HPAEC. The general hydrolysis conditions used were 2 M TFA, for 2 h at 125 °C, unless otherwise stated.

Hydrolysed neutral sugars were analysed by GC-FID as their alditol acetate derivatives. The reduction and acetylation of the alditol acetates is described in Appendix 1.3. Neutral sugars assayed by HPAEC were detected by PAD. Uronic acids were analysed by HPAEC-CD.

2.2 Methylation analysis

The chemical structures of carbohydrates are largely responsible for their functions. The first step to understanding the primary structure of carbohydrates is to determine how the sugar residues are linked. Methylation analysis by GC of partially methylated alditol acetate derivatives of sugars is the most widely used method. Even though several changes and improvements have been made on derivatisation techniques, the basic methodology has remained the same.^{31,32}

All free hydroxyl groups, i.e. those not involved in ring formation, glycosidic linkages or carrying substituents on the sugar polymer, are methylated and upon hydrolysis, the unmethylated hydroxyl groups reveal the positions of linkage. Upon reduction of the anomeric carbon to their equivalent alditol and acetylation of the remaining carbons, detection of which carbons participate in the ring and linkages, is made possible.^{31,32}

Linkage information obtained depends greatly on homogeneity of the material; therefore some preliminary purification steps are necessary. A limitation of the technique is that sequence information is not directly revealed. Backbone composition, linkage and frequency of branching can be directly known. However, if repeating units are present on the polymer, then some further work has to be done. For e.g. digestion by specific enzymes and the use of more modern techniques, such as ¹³C NMR and ¹H NMR, may be of assistance in deriving sequence information.³¹

Neutral and amino saccharides are generally freely soluble in solvents for methylation, e.g. DMSO, while other saccharides only become soluble upon addition of alkali, e.g. NaOH. The advancement of coupling GC with different methods of detection, e.g. GC-FID and GC-MS, has allowed comprehensive analysis of material in as small quantities as 0.2 µg.^{31,31a}

The method of methylation as described by Dell *et al.* was followed for investigating the *Agave americana* heart water extract (Appendix 1.4).³³ Samples were dissolved in a DMSO-NaOH slurry and the methylating agent used was methyl iodide. In order to preserve the integrity of the fructose molecules, very mild hydrolysis conditions of 0.5 M TFA at 60 °C for 1 h were used. The reduction and acetylation procedure followed for the methylated sugars were as described in Appendix 1.3. The PMAA samples were analysed by GC-FID and GC-MS.

2.3 Size-exclusion chromatography

SEC, also called molecular or gel chromatography, is still the most popular method in the analysis of polymers to determine molecular mass distributions, (MMD). It is based upon solute molecules being eluted in order of decreasing molecular size from a stationary phase consisting of a porous, three-dimensional network. The rate at which molecules elute through the molecular sieve depends on the extent to which solute molecules penetrate the pores of the stationary phase. This depends on the ratio of their molecular dimensions to the average diameter of the pores. This technique also applies to obtaining the molecular weight distributions of proteins, enzymes, nucleic acids, peptides, and hormones.³⁴⁻³⁶

SEC analysis was carried out on the different extracts of *Aloe ferox* and *Agave americana* on the columns packed with Sephacryl (poly([allyl dextran]-co-N'N-methylenebisacrylamide)) or Biogel stationary phases. Both Sephacryl (columns 1 and 2) and Biogel (column 3) are chemically inert molecular-sieve gels made of polyacrylamide. They are insoluble in water and organic solvents. This inert nature of the gel also helps decrease the chance of adsorption of polar solvents and can be applied to a wide pH range (pH 2 to 11) of solvents.³⁶

Column 1: Sephacryl, S-400-HR 62 x 1.5 cm, eluent 50 mM potassium-phosphate buffer at pH 6.58 with 0.1 M NaCl, fractionation range 10 – 2000 kDa, void volume (V_o) = 40 ml, total volume (V_t) = 140 ml. The column was calibrated using dextran standards of molecular weights: 500 000, 150 000, 110 000, 70 000 and 10 000 Da. The calibration curve is shown in Figure 2.1. The 10 000 Da falls beyond the linearity region. This can be attributed to the type of buffer used, temperature or the ageing of the matrix.

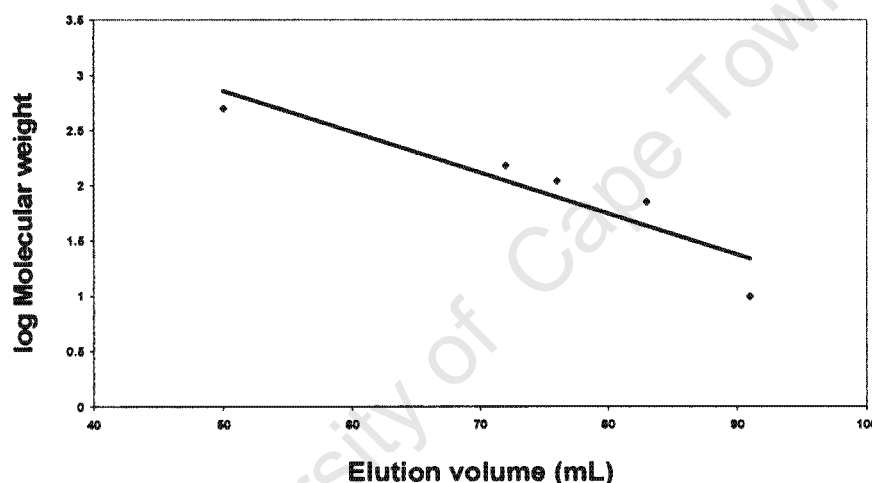


Figure 2.1: Calibration of column 1 (Sephacryl S-400-HR)

Column 2: Sephacryl, S-100-HR 95 x 1 cm, eluent 50 mM potassium-phosphate buffer at pH 6.58 with 0.1 M NaCl, fractionation range 1 – 1000 kDa, void volume (V_o) = 20 ml, total volume (V_t) = 66 ml

Column 3: Biogel P2 95 x 1 cm, eluent water, fractionation range 0.1 – 1.8 kDa, void volume (V_o) = 24 ml, total volume (V_t) = 58 ml

Fractions were monitored by the phenol-sulphuric and carbazole assays.^{29,30}

2.4 Analysis by gas chromatography

GC is a highly versatile method of quantitative and qualitative analysis of a wide range of materials, in all fields of science. Separation in this technique is based upon the rates at which the vapourised components of a mixture are carried through an immobilised stationary phase by an inert gaseous mobile phase. The solute and solvent molecules interact by adsorption.³⁷

GC coupled with detection by FID and MS was employed in the investigation of monosaccharide and linkage composition by identification of alditol acetates and partially methylated alditol acetates.

MS is an analytical technique to characterise molecules based on the measurement of molecular mass. The three essential components that make up a Mass Spectrometer are the ion source, the mass analyser and the detector.^{38,38a}

The ion source ionizes the sample usually by the loss of an electron to form a cation. The main function of the mass analyser is to separate ions according to their mass-to-charge (m/z) ratio. The detector monitors the ion current and a signal is recorded in the form of a mass spectrum. The m/z values of the ions are plotted against their intensities to show the number of species present in the sample, the molecular mass of each component and the relative abundance of the different species. The fragmentation patterns shows peaks corresponding to the loss of specific fragments in a molecule, hence imparting structural information.^{38,38a}

Analysis of *Aloe ferox* alditol acetate samples were carried out by GC-FID isothermally on a *Varian 3300* at 219°C (fitted with a *Teknokroma* TRB-225 capillary column, 30 m long and 0.32 mm wide) with nitrogen as the carrier gas. The PMAA samples of *Agave americana* were analysed by GC-MS with an electron impact ion source, on an *Agilent 6890N* at an initial temperature of 100 °C for 1 min, increasing at 35 °C/min to a final temperature of 310 °C. A capillary column (*J&W DB_1 MS*), 30 m long with an internal diameter (i.d.) of 0.25 mm, was employed with helium as a carrier gas. An *Agilent 5973 Inert MS* was used for detection.

2.5 Analysis by high-performance anion-exchange chromatography

HPAEC coupled with PAD has shown a great advancement in the field of carbohydrate chemistry, since the early 1980's. The potency of HPAEC-PAD, now the standard technique for the analysis of carbohydrates, lies in its simple sample preparation as no derivatization is required. Selective and rapid separation mechanisms minimise epimerization or fragmentation of sugars and low limits of detection (ppm) are possible.³⁹

Ion-exchange resins, which are usually high-molecular weight polymeric materials, containing many ionic functional groups per molecule, serve as the stationary phase. Pellicular anion-exchange resins (positively charged beads) have been specifically designed for carbohydrate analysis by the *Dionex Corp* since decomposition of traditional silica based resins occurs at high pH. Neutral sugars ($pK_a > 12$), become ionized to oxyanions under the strong basic conditions used and can then bind to the positively charged resin beads. The sugar is eluted off the column by an ion exchange mechanism.³⁹

There are several separation mechanisms – the three most important being (1) effective charge of the molecules, (2) their pK_a values and (3) steric effects. The affinity of a molecule to an anion exchanger column is proportional to the number of oxyanions on the molecule. Under alkaline conditions, the order of elution is monosaccharides < oligosaccharides < polysaccharides.³⁹

The affinity of an anionic functional group for an anion exchanger column is inversely proportional to the pK_a value of the functional group. Hydroxyl groups on monosaccharides have differing acidities depending on the nature of their linkage, thereby generating different affinities. The anomeric hydroxyl group has a much lower pK_a value than other hydroxyl groups and therefore reduced saccharides and cyclic glycans elute earlier than their non-reduced and linear counterparts respectively.³⁹

Apart from the influence of pK_a values, the accessibility of oxyanions on the sugars to the functional groups on the stationary phase has a steric influence on separation. Bulky side-chains on sugars can mask the ionic attraction between the resin and saccharide and cause reduced retention times.³⁹

PAD permits detection of hydroxylated species, by means of oxidation of the sugar on a working gold electrode. Sugar nucleotides and sugar phosphates have low PAD responses and are detected by conductivity detection (CD). CD is accomplished by the change in concentration of the eluent, which results in changes in background conductivity, as the anionic species of the eluent compete with the analyte ions for sites on the resin.⁴⁰

HPAEC analysis was carried on the different extracts of *Aloe ferox* and on the water extract of *Agave americana* on a Dionex platform comprising of an AS50 autosampler, LC30 oven, EG50 eluent generator, ED50 electrochemical detector and a GS50 gradient pump. Hydrolysates of *Aloe ferox* extracts were analysed on a CarboPac PA20 column and eluted with 6 mM KOH at a flow rate of 0.5 mL/min. The *Agave americana* water extract hydrolysate was analysed on a CarboPac PA10 column and eluted with 16 mM NaOH at a flow rate of 0.22 mL/min. Qualitative identification of monosaccharides was done based on comparison of relative retention times of standards (Rha, Ara, Gal, Glu and Man) and quantitative analysis was based on relative peak area. A chromatogram of one of the standard runs is shown in Figure 2.2.

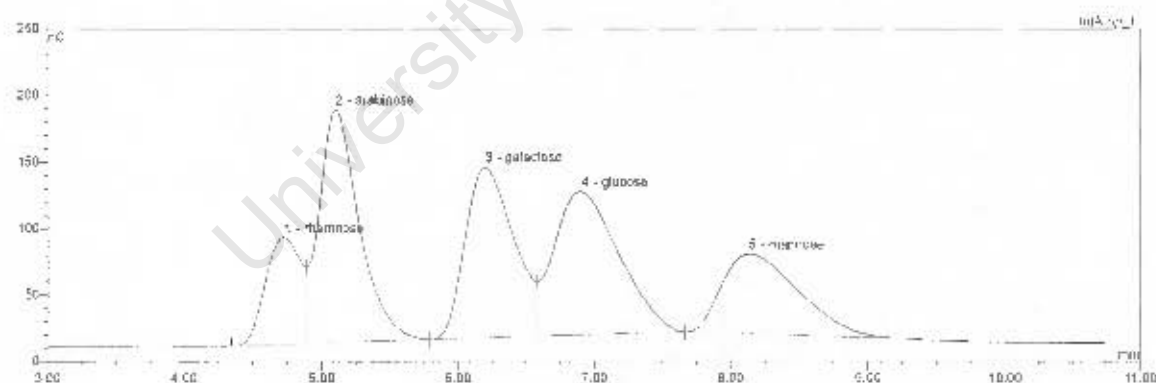


Figure 2.2: Chromatogram of standards on CarboPac PA20 column.

2.6 Nuclear magnetic resonance spectroscopy

Nuclear magnetic resonance (NMR) spectroscopy has a number of advantages that makes it a favoured technique in investigating the molecular structure of organic materials. One great advantage, which is common with other physical methods, is that it is a non-destructive method and samples can be recovered without any modification. NMR analysis is not restricted to the analysis of solutions but also extends to the solid samples.⁴¹⁻⁴³

Analysis by NMR yields spectra of magnetic sensitive nuclei (e.g. ^1H and ^{13}C) which depend on the structural environment of the nuclei. The proton and carbon spectra provide fingerprints which can be used to determine the identity and purity of samples. Confirmation of the assignments of these resonances and unambiguous determination of molecular structure follows from the use of 2D NMR correlation spectra.^{41,42}

The ^1H NMR requires the least amount of sample and forms the starting point in the structural analysis. The chemical shift of a proton depends on its electronic environment and is expressed relative to tetramethylsilane (TMS). The oligosaccharides are investigated as deuterium-exchanged samples; hence each signal arises from a C-linked proton and the chemical shift value depends on its electronic environment. It can be regarded as a distribution of protons according to their electron density. Peaks on the left side of the spectrum are 'downfield' and arise from protons of low electron density, whereas peaks upfield are due to electron-rich protons. The splitting of the peaks is due to spin-spin coupling with neighbouring protons and under optimal conditions, the relative intensities of the signals may correlated to the amount of nucleic producing the signals. However, in both ^1H NMR and ^{13}C NMR studies, the chemical shift values of compounds are affected significantly by changes in solvent, temperature and pH.⁴¹⁻⁴³

There are three main regions in the proton spectrum of carbohydrates: (1) the anomeric region (5.5-4.9 ppm for α -anomers and 4.9-4.3 ppm for β -anomers), (2) the ring proton region (4.5-3.0 ppm), and (3) the high field region where the shielded methyl groups appear.^{42,44}

The ^{13}C NMR spectra are recorded with proton-decoupling and give rise to much simpler spectra. Chemical shift depends on the electronic environment of the atom. In the ^{13}C NMR spectrum, peaks 'downfield' are from carbon atoms of low electron density and peaks found 'upfield' are from electron-rich carbon atoms. The positions of the ^{13}C NMR signals are relatively characteristic and more amenable to assignment by inspection than those of protons. Comparison of ^1H and ^{13}C NMR data with literature values of model compounds permits identification of sugar components and their linkages (from glycosylation shifts). The chemical shifts of peaks are referenced relative to TMS.⁴¹⁻⁴³

In the ^{13}C NMR spectrum of sugars are recorded from 0-200 ppm and there are three main distinguishable regions: (1) carboxyl and carbonyl groups (~170 ppm), (2) anomeric carbons (110-90 ppm), and (3) the remaining ring carbon atom (80-65 ppm) and primary alcohols (65-60 ppm).^{42, 44}

In the 1D analysis of sugar molecules, the anomeric region is of greatest importance. The chemical shift of the anomeric carbon is related to the configuration and substitution of the sugar residue. The multiplicity and peak intensity of the signal is indicative of the relative ratios of the constituent sugars. The resonances of carbon atoms involved in linkages are shifted downfield while the adjacent carbons are shifted upfield. Substituents on the hydroxyl groups of the ring protons also lead to a downfield shift of the adjacent protons.⁴¹

In order to further resolve the ^1H and ^{13}C assignments for identification of sugar residues, their anomeric configuration, and possible position of their linkages, 2D NMR experiments were employed. The 2D experiments carried out were: proton-proton chemical shift correlation spectroscopy (COSY) and proton-carbon heteronuclear chemical shift correlation spectroscopy (HETCOR). The 2D pulse sequences are made up of one or multiple pulses and delays prior to the final observation of the signal. The output of 2D spectra is in the form of a contour plot with frequency axes. Both axes are connected by scalar coupling (homo- or heteronuclear) and give chemical shift information.^{42,43}

COSY spectra consist of a complex diagonal with pairs of off-diagonal peaks which arise from each pair of scalar coupled protons. The coupling of sugar residues can be worked

out starting from a single unambiguous assignment (e.g. H1). Multiple relay COSY can be used to resolve ambiguities arising from overlap of proton resonances.^{42,43}

HETCOR maps contain ^1H chemical shifts along one axis and ^{13}C chemical shifts along the other axis. The peaks on the map arise due to connections between a ^{13}C nucleus and a proton. HETCOR can be used to investigate various types of connectivity e.g. one-bond coupling, long-range couplings or relayed correlation.⁴³ There are basically two types of experiments in this category: Those that utilize multiple quantum transitions during the evolution time (like HMQC, HMBC) and those using single quantum transitions during the evolution time (like HSQC). HSQC experiments correlate protons with their directly attached heteronuclei.

Samples for NMR analysis are prepared by repeatedly dissolving in D_2O and drying. NMR spectra were acquired in D_2O and recorded at 300, 400 and 600 MHz at 30 and 70 °C. NMR spectra were processed using standard Varian software.

3 *Aloe ferox*

The polysaccharides found in *Aloe ferox* leaves have previously been found to be largely pectic in nature and are well known for their gelling properties.^{45,46} However, the present study focuses on the non-pectic water-soluble saccharides in *Aloe ferox* parenchyma in order to compare chemical structure with the commercially produced acemannan derived from in *Aloe vera*. If similar, then *Aloe ferox* may have the same beneficial physical and immunomodulatory properties as *Aloe vera*.

3.1 Processing of *Aloe ferox* raw material

The *Aloe ferox* leaves used in this work were harvested in Graaff Reinet from plants growing in the wilderness. Plants were supplied and identified by Roy McJachlan, Managing Director, Agave Distillers (Pty) Ltd. In addition, leaves from an old dehydrated plant and a young cultivated plant, both grown in Cape Town, were harvested for a comparative study.

The experimental procedure followed for the processing of the Graaff Reinet leaf portions is illustrated in Figure 3.1.

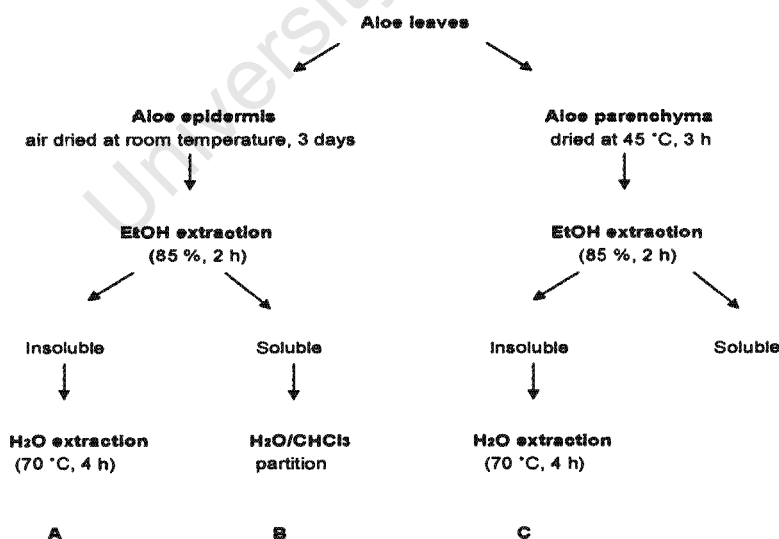


Figure 3.1: Flow diagram of experimental procedure followed

Whole leaves, obtained from Graaff Reinet, were between 30 and 60 cm long. The leaves were washed with tap water to remove residual surface dirt prior to removing the thorns along the margins. Thereafter, the green outer layer (epidermis) was separated from the inner white portion (parenchyma), using a knife. Both portions were washed with tap water to remove the yellow exudates (aloin bitters) and kept at room temperature for no longer than 1 h until drying.

The fresh aloe parenchyma tissues were cut into strips (~ 5 x 0.5 x 0.5 cm), and dried in a tunnel-dryer at 45 ± 2 °C for 3 h. The final moisture content of the dried parenchyma was found to be approximately 8 %. The strips were milled in a hammer-mill using a 0.5 mm sieve to give evenly textured and uniformly sized particles. The *Aloe ferox* epidermis was cut into strips (~ 1 x 0.5 x 0.5 cm) and dried in an incubator room (~ 30°C) for 3 days.

The dried aloe epidermis and parenchyma portions were immersed into boiling ethanol [85% (v/v) aqueous] for 1 h, to defat and dissolve low-molecular weight sugars. The alcohol insoluble residues (AIRs), of the aloe epidermis and parenchyma then underwent extraction in hot water (70 °C) for 4 h with agitation, to give extracts A and C respectively (as depicted in the flow diagram). The water extracts were centrifuged to remove the insoluble particulate matter and the soluble portion was freeze-dried prior to further analysis. Only the water-soluble extracts of *Aloe ferox* were investigated as these readily obtained extracts would be of commercial interest.

The ethanol extract of the epidermis was further partitioned between chloroform and water, and the aqueous layer (B) was retained for analysis. After freeze-drying, extracts A, B and C were granular and off-white to yellow in colour.

3.2 Size and composition analysis of water-soluble epidermis extracts A and B

3.2.1 Size analysis of extracts A and B

SEC analysis was carried out on the water-soluble components of the *Aloe ferox* epidermis extracts (A) and (B), on column 1 (Sephacryl S-400-HR) and fractions were screened by use of a phenol-sulphuric assay. The molecular mass profile of extract A is shown in Figure 3.2.

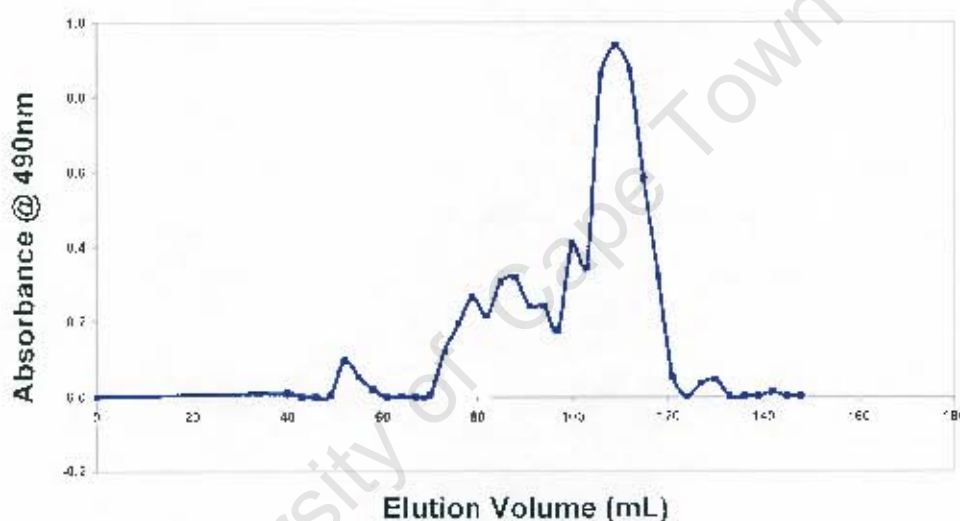


Figure 3.2: Molecular mass distribution of saccharides in extract A

Extract A, the water extract of the epidermis, shows the presence of a range of polymer sizes, with only a small percentage of high-molecular weight polysaccharides (~ 500 kDa) and a higher proportion of low-molecular weight material (~ 10 kDa).

The molecular mass profile of extract B is given in Figure 3.3.

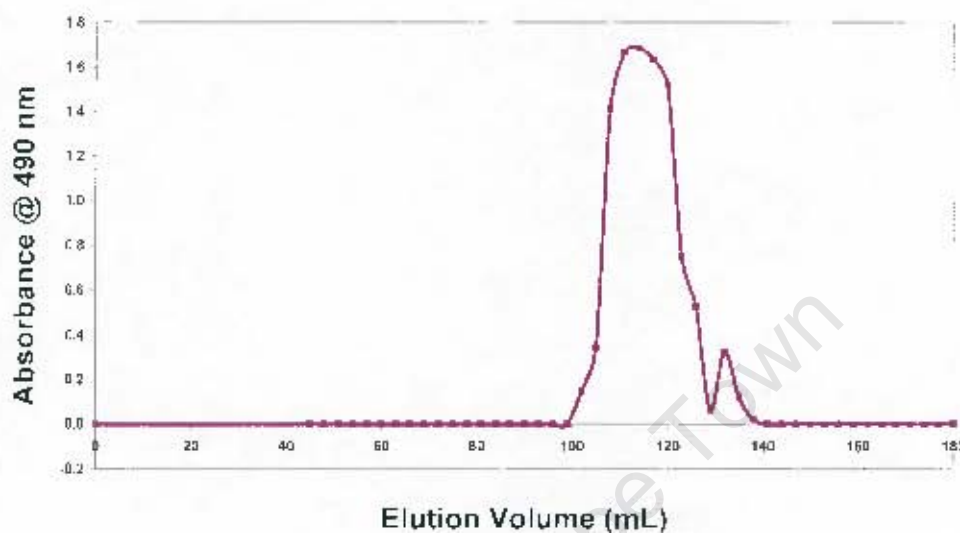


Figure 3.3: Molecular mass distribution of saccharides in extract B

Extract B only contained material eluting at the total volume (≤ 10 kDa). This result was predicted for B as the 85 % ethanol used during the AIR preparation was expected to remove lipids and low-molecular weight sugars from the sample. During the partitioning between CHCl_3 and water, the lipids would have dissolved in CHCl_3 leaving the monosaccharides and small oligosaccharides in the aqueous layer.

In the SEC analysis of extract A and B, the low-molecular weight material elutes well beyond the linear region of the calibration curve. This can be attributed to either a very low hydrodynamic volume of the material or to some interaction of the sample with the matrix.

3.2.2 Composition analysis of extracts A and B

The monosaccharide composition of extracts A and B was determined by HPAEC-PAD, (Section 2.5). Hydrolysis was carried out with 2 M TFA at 125 °C for 2 and 4 h respectively. The results of the assays are illustrated in Figures 3.4 and 3.5.

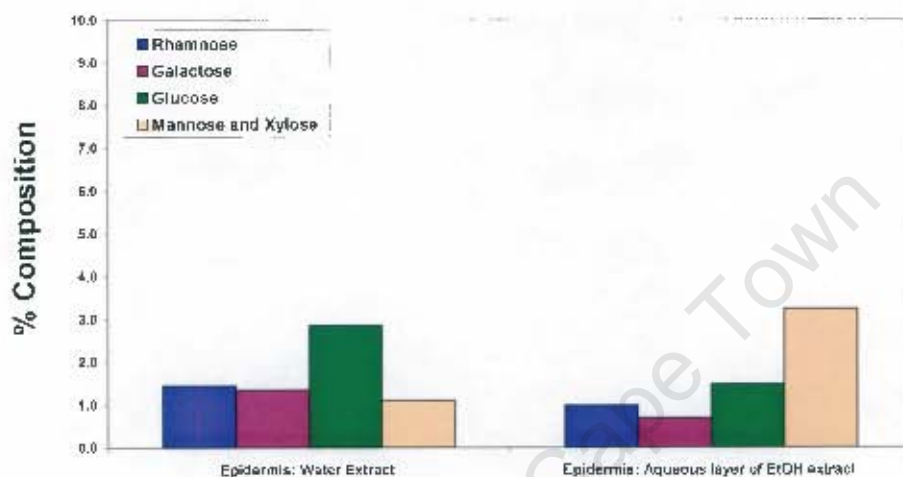


Figure 3.4: Monosaccharide percentage composition in extracts A and B after hydrolysis (2 h)

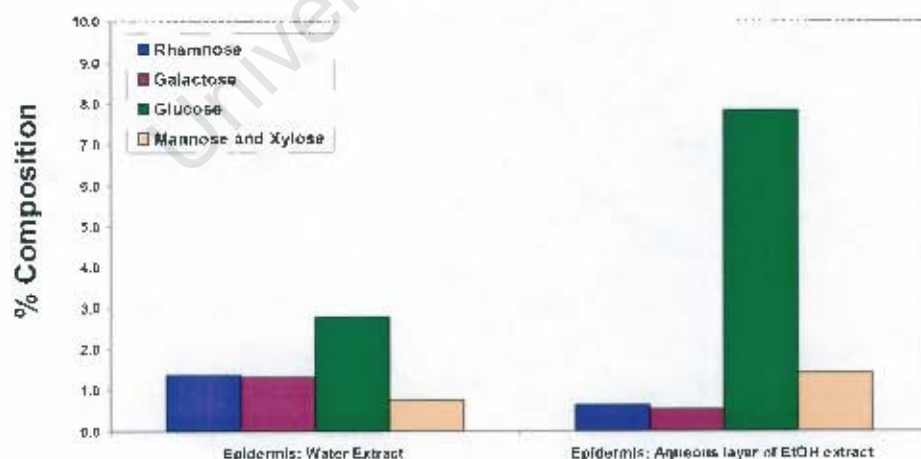


Figure 3.5: Monosaccharide percentage composition in extracts A and B after hydrolysis (4 h)

Extract A had a similar profile following the hydrolytic periods of 2 and 4 h. However, extract B showed an increase in the release of glucose after hydrolysis for 4 h. As SEC results show that extract B is of relatively low-molecular weight material, the increase in glucose could be attributed to a more complete hydrolysis of small chain polymers.

However in both fraction A and fraction B, the percentage of total sugar recovered relative to the amount of starting material hydrolysed was very low. Recovery of sugar was measured based on the internal standard added to the analysis. This could be explained by the presence of pectic material in the water-soluble extracts that is not measured, as this assay detects only neutral saccharides and not uronic acids. Further analysis was not carried here as the parenchyma part of the plant was of interest.

3.3 Size and composition analysis of water-soluble parenchyma extract C

3.3.1. Size analysis of extract C by SEC with carbohydrate and uronic acid analysis

Extract C, the water-soluble extract of *aloe* parenchyma, is the material of interest as it is expected to contain the high-molecular weight functional polysaccharides purported to have the many healing properties reported for *Aloe vera*. The molecular mass profile of extract C is shown in Figure 3.6. The sample was eluted through column 1 (Sephacryl S-400-HR) and fractions were screened by use of a phenol-sulphuric assay.

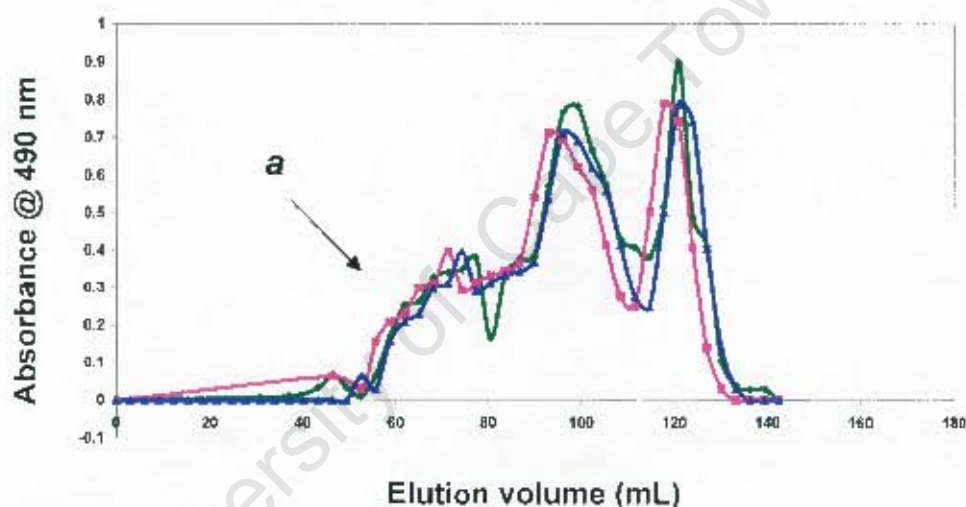


Figure 3.6: Molecular mass distribution of polymeric material in extract C

The repeated runs show similar profiles in the size distribution of polymers. Three distinct peaks can be seen in the elution ranges of 40-75 mL, 78-100 mL and 103-140 mL respectively. The molecular sizes that correspond to these elution volumes are ≥ 500 , 110-70 and ≤ 10 kDa, hence a wide distribution in the size of saccharides.

Since high-molecular weight polysaccharides from *Aloe vera* have demonstrated maximum immunomodulatory activity, peak a (molecular weight ≥ 500 kDa), as shown in Figure 3.6, was isolated for further analysis. Peak a is least likely to be pectin as only water was used for the extraction, and high-molecular weight pectic polysaccharides would require harsher conditions to be extracted.⁴⁵ Material collected after several runs

was pooled and dialysed overnight against water to remove the phosphate salts. The freeze-dried material was analysed by HPAEC-PAD, (Section 2.5). Results from HPAEC-PAD analysis showed the presence of mannose, glucose and galactose. The ratio of mannose to glucose was 3:1 but very low levels of sugar were detected.

Work carried out on *Aloe vera* has shown that heat treatment affects the average molecular weight of neutral and acidic polysaccharides. The average molecular weight of purified acemannan, the main bioactive polysaccharide in *Aloe vera*, notably increased as the drying temperature increased. A freeze-dried sample of acemannan was found to be approximately 45 kDa, and the average molecular weight of samples dehydrated at temperatures between 30 and 50 °C was found to be in a similar range. However, as the drying temperature of the samples increased, the average molecular weight significantly increased as well. The average molecular weight of samples dried at 70 and 80 °C increased up to 75 and 81 kDa respectively.⁹ Acemannan has an O-acetylated glucomannan backbone. The polymer is branched at O2, O3 and O6 of 1,4 linked β -Manp chain to single α -Galp side chains. A possible explanation for this observation can be due to loss of terminal galactosyl residues and deacetylation at higher temperatures. This may have caused hydrogen bonding between different mannose chains leading to aggregation and a higher apparent molecular weight.

The *Aloe ferox* parenchyma tissues employed in this study were dried at 45 °C and as temperatures in this range have minimal effect on physical properties of the polymer of *Aloe vera*, it was assumed *Aloe ferox* would behave in a similar way.

In order to assay the pectic content of the soluble polymers in extract C, a carbazole assay was run parallel to the phenol-sulphuric assay. The profiles are shown in Figure 3.7. The sample was eluted on column: 1 (Sephacryl S-400-HR) under the same conditions (buffer and flow rate) previously used, but the column length was shorter hence a lower total volume (V_t). (Section 2.3)

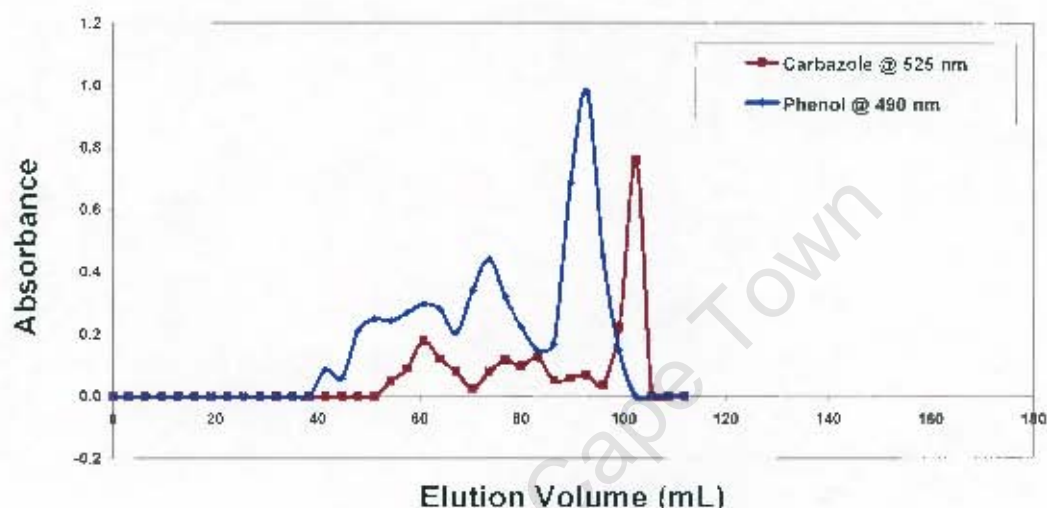


Figure 3.7: Comparison of phenol-sulphuric and carbazole assays of extract C

A fairly similar profile existed in the phenol-sulphuric and carbazole assays, which may be partially due to cross reactions between the two tests. These profiles were similar in that the range of molecular size of the molecules was alike. A higher percentage of low-molecular weight carbazole positive molecules were detected and indicate that the smaller pectic molecules were more easily extracted by hot water.

3.3.2. Composition analysis of extract C by HPAEC

According to literature, the chemical composition of aloe plants is largely dependent on the species analysed, the geographical origin of the plant and the different parts of aloe plants, namely the epidermis and the parenchyma.⁶ Studies on *Aloe vera* parenchymatous tissue have shown that apart from a very high water content (98.5 to 99.5 %), the remaining solid material is made up mostly of polysaccharides (> 60 %), which are highly water soluble.⁸

HPAEC-PAD analysis was carried out in duplicate on extract C after a 2 and 4 h hydrolysis period using 2 M TFA at 125 °C. As indicated in the introduction, the active polysaccharide present in *Aloe vera* is acemannan, a mannose rich polymer which has a mannose to glucose ratio of 15:1. The results from this experiment showed the presence of rhamnose, galactose, glucose and mannose in extract C after both the 2 and 4 h hydrolysis period. However, after the 4 h hydrolysis period, there was a 5 % increase in the amount of glucose released and although there was an increase in the total amount of sugar assayed, the recovery was still low (~ 10 %).

From reports in literature, the preferred acid concentration for hydrolysis was 2 M, but hydrolysis times varied. This led to further trials where extract C was hydrolysed with 2 M TFA for 2, 4 and 8 h at 125 °C. The chromatograms of the HPAEC-PAD analysis are shown in Figures 3.8-3.10 and the data is illustrated in Figure 3.11.

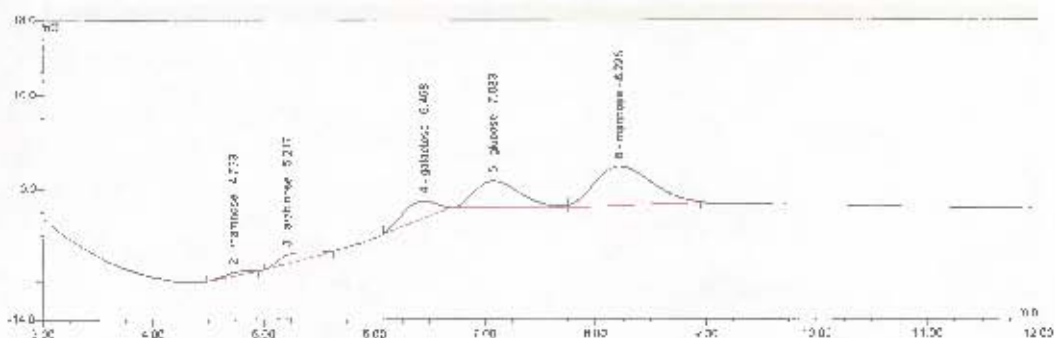


Figure 3.8: Monosaccharide percentage composition in extract C after a 2 h hydrolysis period

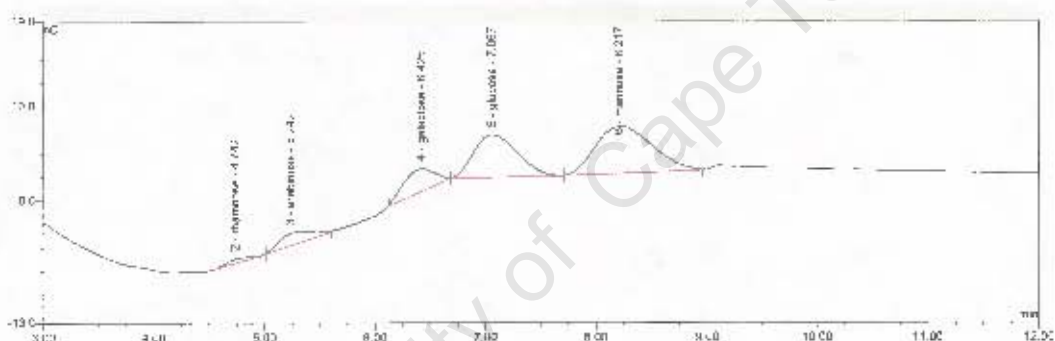


Figure 3.9: Monosaccharide percentage composition in extract C after a 4 h hydrolysis period

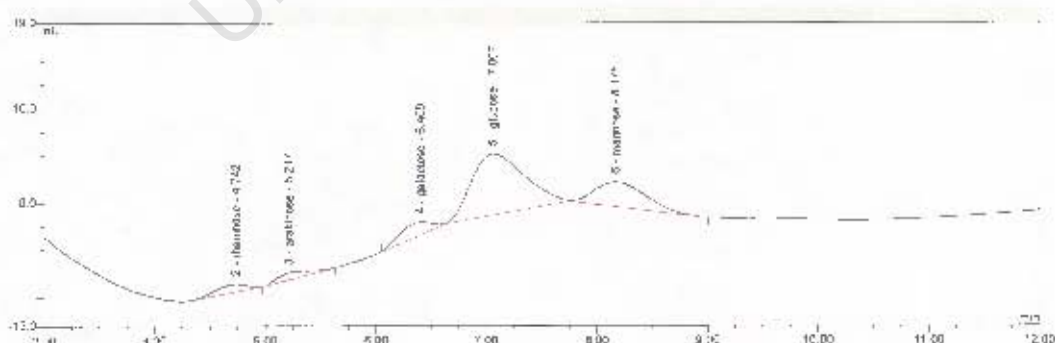


Figure 3.10: Monosaccharide percentage composition in extract C after an 8 h hydrolysis period

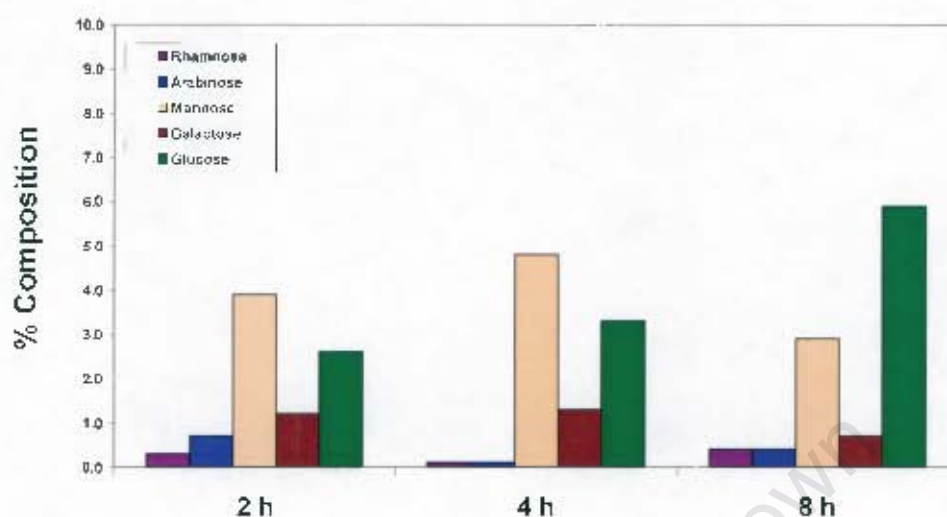


Figure 3.11: Monosaccharide percentage composition in extract C after different hydrolysis periods

The results show an increase in the total amount of carbohydrate assayed (8.7, 9.6 and 10.3 %) after the hydrolysis periods of 2, 4 and 8 h respectively. After hydrolysis for 2 and 4 h, mannose and glucose were found in a ratio of approximately 3:2. However, after hydrolysis of 8 h, the percentage of mannose decreased, as illustrated in Figure 3.11. There was a steady increase in the amount of glucose as hydrolysis times increased. This long period of hydrolysis appears to have destroyed mannose but has favoured the release of glucose.

Research done on the bioactive polysaccharide found in *Aloe vera*, acemannan, found that heat treatment had a remarkable effect on the composition of the polysaccharide.⁶ Drying at temperatures even as low as 30-40 °C caused a significant loss of uronic acids and neutral sugars when compared to a sample that was just freeze-dried. Drying at temperatures up to 50 °C has caused loss of sugars between 11.3 to 14.1 %.⁹

When parenchyma tissues were dried at 70 °C, a 20.7 % loss of sugars was detected. Another interesting feature of this study is that mannose units were lost in the greatest percentage when the drying temperatures were increased. Galactose showed the second greatest loss.⁹ The decrease in mannose units may be due to deacetylation of

the polysaccharide backbone, which may have caused in hydrogen bonding between the different mannose chains to result in an acid-resistant form of the polymer.⁹ The *Aloe ferox* parenchyma tissues employed in this study were dried at 45 °C and drying at this temperature may have caused some impact on these results.

University of Cape Town

3.4 Additional compositional studies

The dried and milled parenchyma material, extract B and extract C, were assayed by phenol-sulphuric and carbazole assays to detect the levels of neutral and charged polysaccharides. Prior to analysis, the dried and milled parenchyma material was hydrolysed by Seaman Hydrolysis (12 M H₂SO₄ for 3 h at room temperature), to break down cellulose. This was done in order to obtain a more accurate estimation of the carbohydrate content using the phenol-sulphuric assay, and to compare with the literature values of the carbohydrate content of *Aloe vera*.⁹ The results of the different experiments are presented in Table 3.1.

Table 3.1: Carbohydrate composition of *Aloe ferox* leaves

	[†] Carbohydrate % (w/w)	[*] Uronic acid % (w/w)
Aloe parenchyma (dried and milled)	54.1	21.6
Water extract (C)	8.3	6.5
Aqueous fraction of EtOH extract (B)	8.2	n.d

[†] Samples assayed by phenol-sulphuric assay

^{*} Samples were assayed by a carbazole colorimetric test

Hydrolysis conditions:

Aloe parenchyma – hydrolysed in 12 M H₂SO₄ for 3 h at room temperature;

Water extract in 1 M H₂SO₄ for 1 h at 100 °C;

Aqueous fraction of ethanol extract was dissolved in water – not hydrolysed

The carbohydrate content in the dried parenchyma tissue, as measured by use of a phenol-sulphuric assay was found to be ~ 54 %, which is similar to the literature values for *Aloe vera* (~ 60 %).^{9,10} The freeze-dried water extract of the parenchyma and the aqueous fraction of the ethanol extract were similarly assayed and the carbohydrate content measured was ~ 8 % in both cases. At this stage, the water extract was analysed by the use of a carbazole assay for uronic acids, and the uronic acid content was found to be ~ 6.5 %. All the results given are the mean of three measurements of each extract.

Uronic acids are components of pectins which are matrix polysaccharides. They are trapped within the polysaccharide matrix of the plant as they are complexed with Ca^{2+} ions. EDTA was not used to release the Ca^{2+} as the pectic material was not of interest in this project.

At this stage, the results conclusively indicate that the polysaccharides in *Aloe ferox* are poorly water-soluble. Previous work carried out by Mabusela *et al.* on this particular species of *Aloe* indicate that the carbohydrates are mainly pectic material, soluble in aqueous ammonium oxalate and alkali.⁴⁵ In this project and the work carried out by Mabusela *et al.*, the *Aloe ferox* sample preparation and extraction conditions were different, therefore there could not be an absolute comparison of results.

In their experiment, polysaccharide material was sequentially extracted with water, then aqueous $(\text{NH}_4)_2\text{C}_2\text{O}_4$, followed by increasing concentrations of KOH. Prior to the water extraction, the parenchyma underwent extraction in benzene and methanol. Based on mass, the material extracted with water was only 12.5 % of the starting material (fresh parenchyma tissues) compared to the aqueous $(\text{NH}_4)_2\text{C}_2\text{O}_4$ extract which yielded 25 % of the starting material. The carbohydrate content in the water extract was approximately 20 %, whereas in the aqueous $(\text{NH}_4)_2\text{C}_2\text{O}_4$, the carbohydrate content was approximately 70 %.⁴⁵

This earlier work showed that the water-soluble polymers, as determined by a GC assay, were composed of Rha, Ara, Xyl, Gal, Glc and uronic acids in the ratio of 9:10:1:10:3:1. The aqueous $(\text{NH}_4)_2\text{C}_2\text{O}_4$ extract was dominated by a very high uronic acid content compared to neutral sugars, characteristic of the presence of pectic polymers.⁴⁵

Hence *Aloe ferox* cannot be considered as a suitable substitute for *Aloe vera*, in health products for immunomodulatory purposes. There are no significant similarities between the polysaccharides found in *Aloe ferox* and the active polysaccharides found in *Aloe vera*. In *Aloe ferox*, high molecular-weight polysaccharides are not abundant, the polysaccharides are not highly water-soluble and are not rich in glucomannans.^{6,9,10}

3.5 Size analysis of the water extract of ultrasound treated *Aloe ferox* parenchyma

At this stage further processing was attempted in order to disrupt cell structures to release more compounds, as extracting with water at 70 °C appeared not to extract neutral or charged high-molecular weight polymers in significantly large amounts. This occurrence is probably due to interaction of the sugars with the structural compounds of the cell walls. Ultrasound was selected as it has been shown to release carbohydrates and disrupt cell walls.⁴⁷⁻⁴⁹

The dried and milled *Aloe ferox* parenchyma material was added to distilled water and subjected to ultrasound treatment. The following apparatus was used: *Vibracell* 750VCX sonicator with a power output of 20 kHz a standard titanium alloy horn (13 mm) connected to a piezoelectric transducer. The power output at the horn tip was approximately 20 W/cm² at 100 % amplitude. A double-walled glass chamber (96 mm deep) with a diameter of 33 mm was used in a temperature controlled run, reaching a maximum temperature of 40 °C for 10 min. The insoluble residue was removed by filtration and the water-soluble extract was freeze-dried prior to SEC analysis. The water-soluble freeze-dried extract was profiled by SEC on column 1 (Sephacryl S-400-HR) and screened by the use of phenol-sulphuric and carbazole assays. The molecular mass distribution patterns of the neutral and charged saccharides are shown in Figure 3.12.

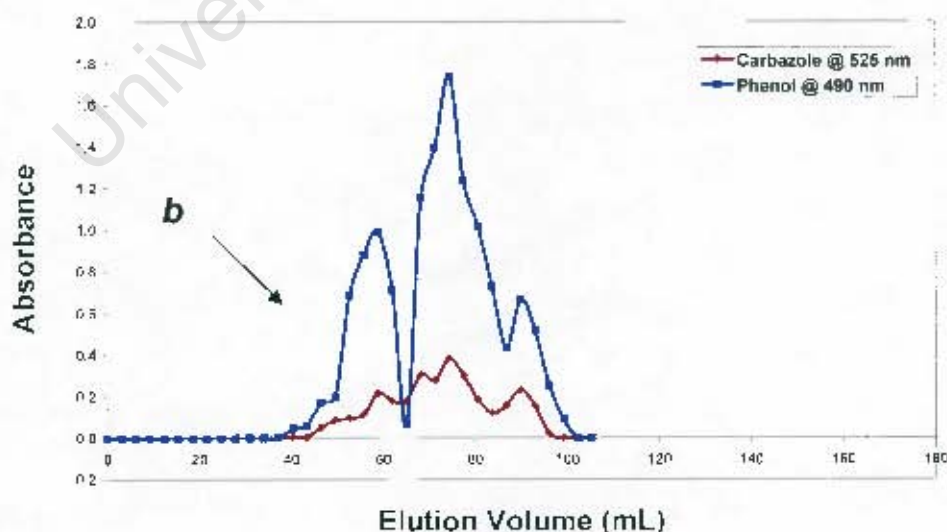


Figure 3.12: Comparison of phenol-sulphuric and carbazole assays of water-soluble *Aloe ferox* parenchyma treated with ultrasound

Comparison of the phenol-sulphuric and carbazole assays of the water extract at 70 °C and the ultrasound treated material, Figures 3.7 and 3.12 respectively, showed a change in the size profile of the polymers. Ultrasonic waves have caused a greater release of high-molecular weight neutral polysaccharides compared to acidic polysaccharides. Peak **b** (≥ 500 kDa), was of interest as it was unlikely to be pectic substances. The peak was isolated after repeated runs and analysed by HPAEC-PAD in order to determine the levels of mannose, galactose and glucose. All three sugars were detected in greater amounts in peak **b** compared to peak **a** (water extract at 70 °C) and the ratio of mannose to glucose was again found to be 3:1 as was for peak **a**, but the total recovery of sugar was still low (< 15 %).

3.6 Comparative study of leaves from *Aloe ferox* trees growing under different environmental conditions

As stated previously, species, geographical origin and environmental conditions impact on the chemical composition of aloe plants.⁹ The *Aloe ferox* leaves employed in this work were obtained from Graaff Reinet in the Eastern Cape and those used in the work done by Mabusela *et al.* were harvested in Albertinia in the Western Cape. The monosaccharide compositions and ratios did differ in the extracts of both leaves; however the experimental procedures followed in the experiments were also different. In order to observe the variation brought about by environmental conditions, a parallel experiment was run with leaves obtained from two different sources.

A batch of leaves was obtained from aloe trees growing alongside the Liesbeek River which were growing under stressed conditions of poor soil and lack of moisture. The leaves were extremely spiky, the parenchyma was dry and leathery and large quantities of yellow bitters (aloin) were present (**Riverside batch**). The second batch, from much younger plants, was obtained from a cultivated garden in Rosebank. These leaves were growing in good conditions and had firm moist parenchyma (**CSIR batch**).

The parenchyma was homogenised and the liquid and cell wall insolubles were separated. The liquid and cell wall insolubles were hydrolysed for 2 h with 2 M TFA and assayed by HPAEC for neutral sugars and uronic acids. The results are given in Table 3.2 and the data is presented in Figures 3.13 and 3.14.

Table 3.2: Monosaccharide percentage composition of the two different extracts of the two batches of leaves

	Rhamnose	Arabinose	Galactose	Glucose	Mannose	Galacturonic acid	Glucuronic Acid
Riverside							
Liquid	0.09	0.12	0.59	4.44	0.79	0.10	n.d.
Cell wall insolubles	n.d.	0.10	1.13	0.81	0.84	n.d.	n.d.
CSIR							
Liquid	n.d.	0.09	0.27	10.17	0.72	0.19	0.01
Cell wall insolubles	n.d.	n.d.	0.09	2.92	0.22	n.d.	n.d.

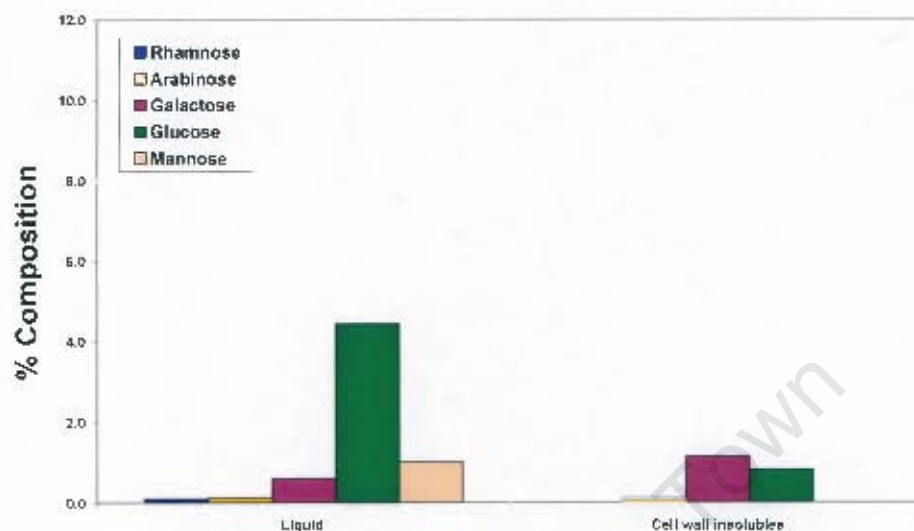


Figure 3.13: Monosaccharide percentage composition of two different extracts of the Riverside leaves

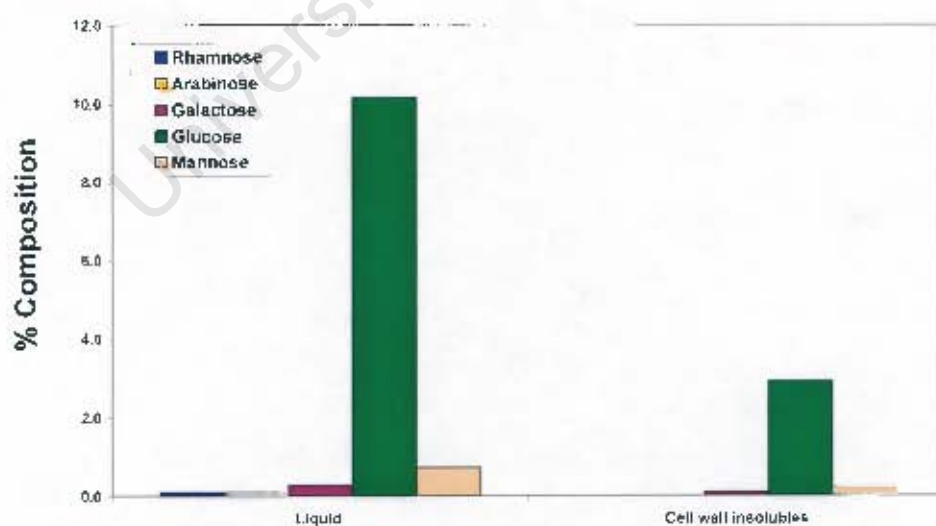


Figure 3.14: Monosaccharide percentage composition of two different extracts of the CSIR leaves

The data (Table 3.2) shows the differences in the monosaccharide composition in the leaves of *Aloe ferox* plants growing under different environmental conditions. The younger CSIR plant has a much higher concentration of glucose compared to the older Riverside plant. This is probably indicative of a 'growing plant' and glucose may be destined for cell wall development.

The total amount of sugar released was greater in the CSIR batch of leaves (26 %), compared to the Riverside batch (15 %). The results confirm that environmental conditions, age and the growth-stage of the plant, do impact on the monosaccharide composition of *Aloe ferox* leaves and may account for the differences in the results obtained from this experiment compared to those obtained by Mabusela *et al.*⁴⁵

3.7 Conclusion

The main objective of this study was to determine the chemical properties, such as molecular size and composition, of the water soluble polysaccharides in the leaves of *Aloe ferox* plants, and to bench mark *Aloe ferox* as a viable substitute for *Aloe vera*.

Results from SEC showed that a range of polysaccharides sizes were present in the water-soluble extract of the *Aloe ferox* parenchyma, with a high percentage of polymers eluting at the total volume, indicating the presence of low-molecular weight polymeric material. Monosaccharide analysis by HPAEC-PAD found that the polysaccharides were composed primarily of rhamnose, galactose, glucose and mannose, but the overall percentages of total sugars recovered were very low, between 10-25 %. When analysing the monosaccharide composition of the water extract, various acid conditions and times were investigated in order to determine the optimal hydrolysis conditions. However, in all experiments it was noted that the water-soluble carbohydrate content was very low and the monosaccharide composition differed from literature results of *Aloe vera*, which consists of polymers rich in mannose. Further structural studies were therefore not deemed necessary.

The water extract was subjected to ultrasound treatment in an effort to try and increase the amount of carbohydrate released; and a comparative study of *Aloe ferox* leaves from different sources to investigate the impact of environmental conditions. Results from these studies showed that ultrasonic waves did release a greater amount of water-soluble material however not sufficiently high relative to *Aloe vera*. The comparative study of leaves shows that environmental conditions (moisture and nutrition) and geographical location does impact the monosaccharide composition of leaves, hence the difference in literature reports.

The overall conclusion from this study is that the polysaccharides in *Aloe ferox* leaves are not highly soluble in water, but are instead soluble in ammonium oxalate indicating pectic material. No glucomannan similar to acemannan could be detected suggesting that *Aloe ferox* cannot be considered a suitable substitute for *Aloe vera* which contains immunomodulatory storage polysaccharides that are readily water-soluble but has good water retention properties for suitable use in beauty products.

which was found to be 17. The remaining complex signals between 4.40 and 3.56 ppm are due to H2 to H6 of glucopyranose and the β -fructosyl residues. These peaks were assigned based on comparison of chemical shifts with literature values and confirmed by use of the proton-carbon correlation (HSQC) experiments.^{19,23,44}

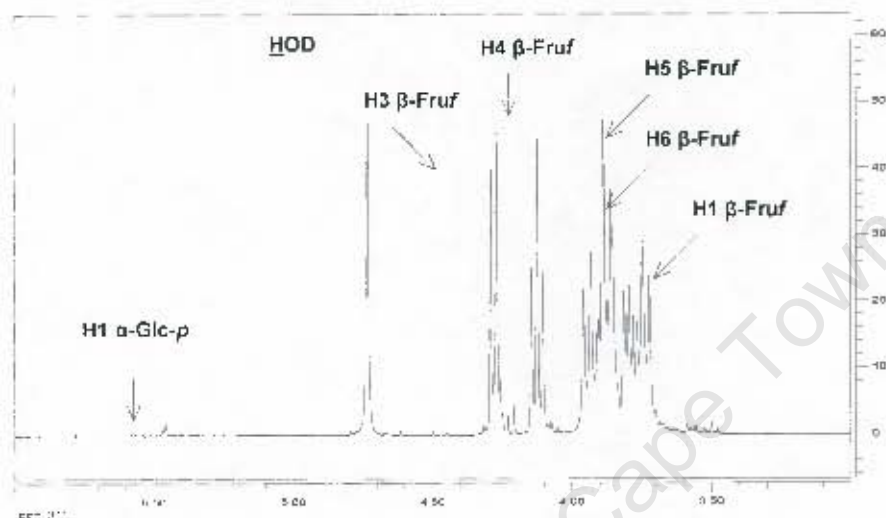


Figure 4.15: ^1H NMR spectrum of chicory inulin

The ^{13}C NMR spectrum of chicory inulin is shown in Figure 4.16, and the assignments are given in Table 4.1.

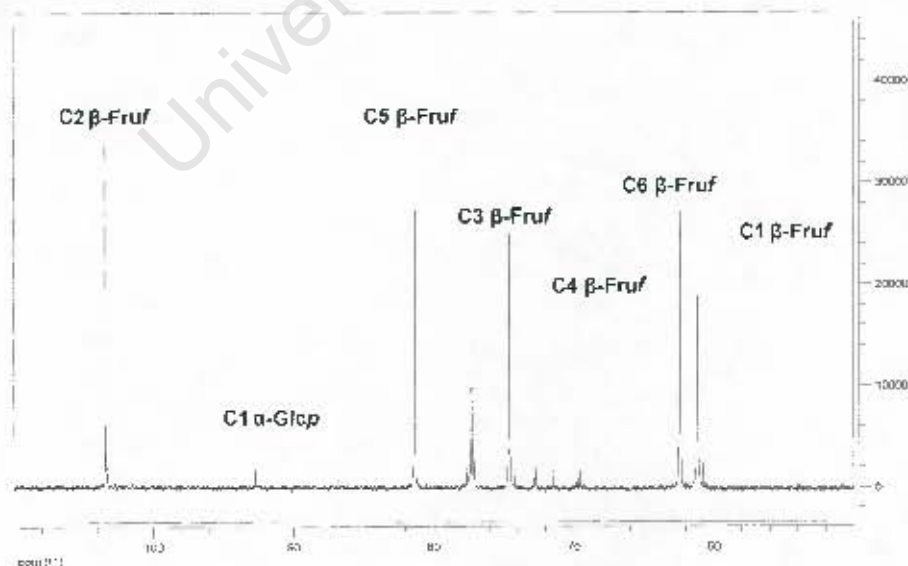


Figure 4.16: ^{13}C NMR spectrum of chicory inulin

The spectrum is dominated by 6 distinct peaks (C1-C6 of fructose) corresponding to the in-chain fructose residues. Glucose signals are much smaller peaks with the anomeric glucose carbon appearing at a chemical shift of 92.71 ppm and the other ring carbons appearing in the region of 74.72 to 70.97 ppm, (Figure 4.16). The assignments of the peak are given in Table 4.1.

Table 4.1: ^{13}C NMR chemical shifts in ppm of the β -D-Fruf and α -D-Glcp units of chicory inulin (Sigma standard) from Figure 4.16.

Carbon		Chicory inulin
Fructose		
C1	(2→1) linked	61.15
	Terminal	60.79
C2	(2→1) linked	104.91
	Glc(1→2)Fru	104.35
	Terminal	105.39
C3	(2→1) linked	77.24
	Glc(1→2)Fru	77.40
	Terminal	77.07
C4	(2→1) linked	74.55
	Terminal	74.15
C5	(2→1) linked	81.31
C6	(2→1) linked	62.35
Glucose		
C1	Terminal	92.71
C2	Terminal	71.45
C3	Terminal	72.85
C4	Terminal	69.50
C5	Terminal	72.68
C6	Terminal	60.40

There are several peaks present for the anomeric carbon (C2) signal of β -Fruf due to the three different environments. Ring carbons engaged in glycosidic linkages are displaced downfield, this deshielding is due to the β -substituent effect. A lesser effect is noted on the adjacent carbons resulting in an upfield shift, this is known as the γ steric effect.⁴² This means that C2 of 1,2-linked β -Fruf will resonate upfield of the 2-linked β -Fruf.

The most abundant peak represents C2 of the internal in-chain fructose residues, which resonates at 104.91 ppm. The resonance at 104.35 ppm, upfield to the principal C2 peak, is due to the anomeric carbon of the fructose residue linked to the terminal glucose residue, which exerts a stronger shielding effect than Fruf. The peak at 105.39 ppm is due to C2 of the terminal fructose residue, which is not subjected to the shielding effect of the substituent at C1. The other ring carbons give signals in the region of 81.31 to 60.79 ppm and have been assigned based on comparison of chemical shifts with literature.^{19-23,44} The two dimensional proton-carbon correlation (HSQC) spectrum of chicory inulin (Sigma standard) is shown in Figure 4.17.

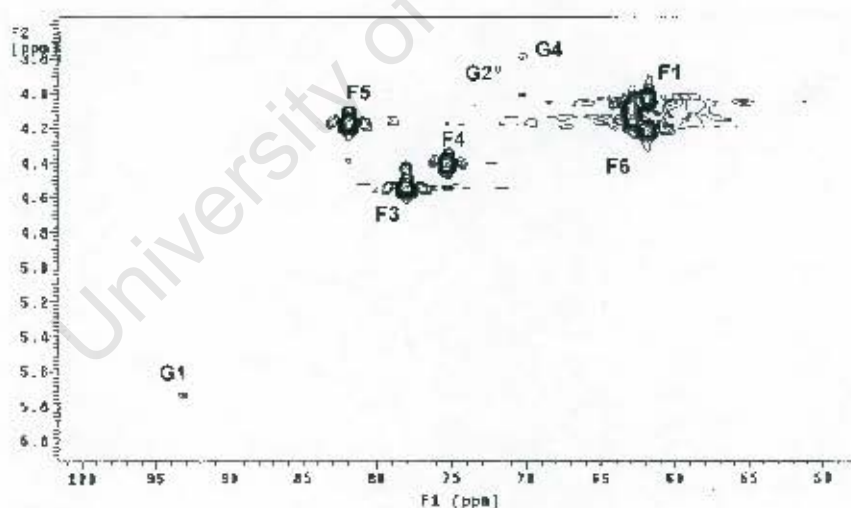


Figure 4.17: The HSQC spectrum of chicory inulin

The major proton-carbon cross peaks have been identified and the assignments agree with the structure of chicory inulin given in literature.

The proton NMR spectrum of the *Agave americana* water extract is given in Figure 4.18.

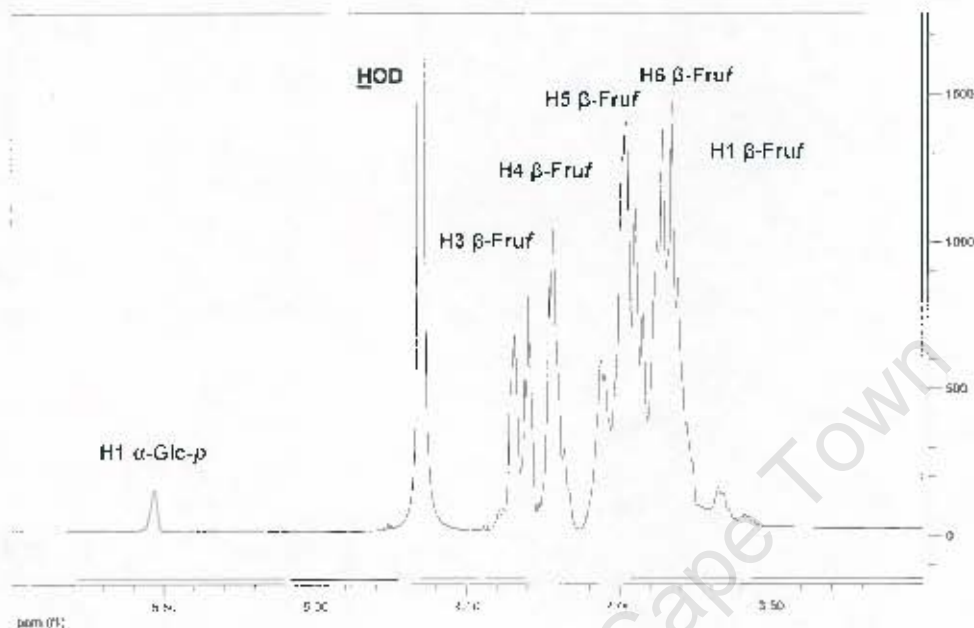


Figure 4.18: ¹H NMR spectrum of the *Agave americana* water extract

The proton spectrum shows that no free fructose or glucose is present as only a single anomeric glucose peak is present. The peak at 5.46 ppm represents H1 of α-glucopyranose. The remaining signals between 4.20 and 3.10 ppm are due to H2 to H6 of glucopyranose and the fructosyl residues.

The average DP estimated by NMR was found to be 16, which is consistent with the average DP estimated by size analysis by HPEAC-PAD.

The ^{13}C NMR spectrum of the saccharides in *Agave americana* is given in Figure 4.19, with an inset of an expansion of the anomeric region.

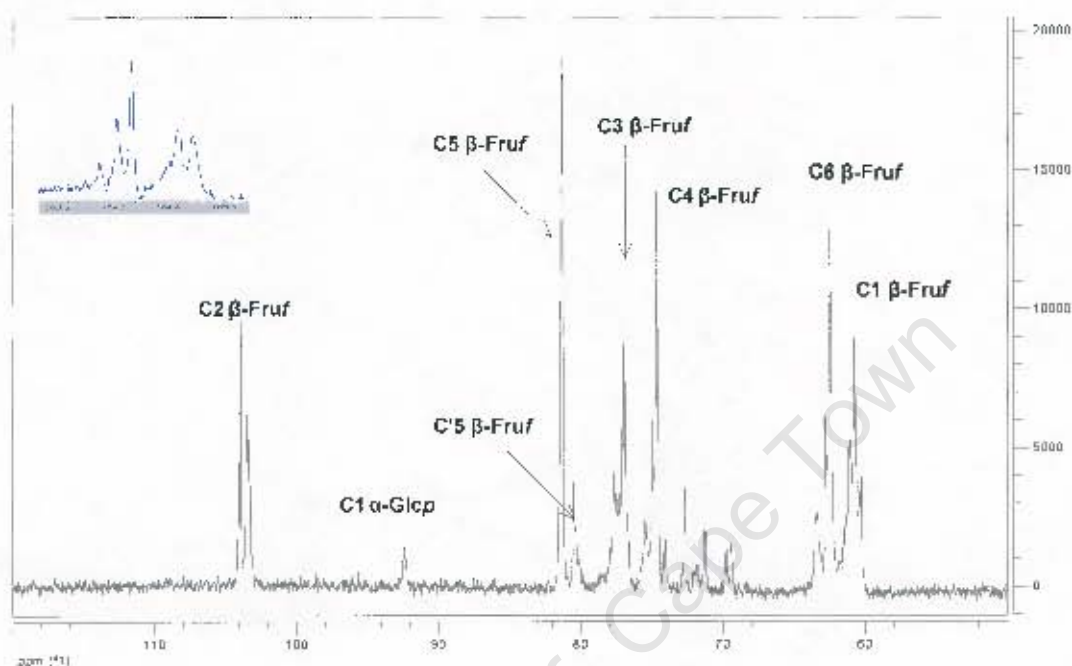


Figure 4.19: ^{13}C NMR spectrum of the *Agave americana* water extract

The spectrum has six dominant resonances (C1 to C6 of fructose), but they appear as several peaks due to the different electronic environments present. This confirms that the structure of the agave saccharide is much more complicated than the linear inulin produced by chicory. The carbon resonances were assigned based by comparison of the chemical shifts of these peaks with the chemical shifts of carbons present in chicory inulin and literature values. Several assignments were confirmed by use of the HSQC spectrum shown in Figure 4.20.

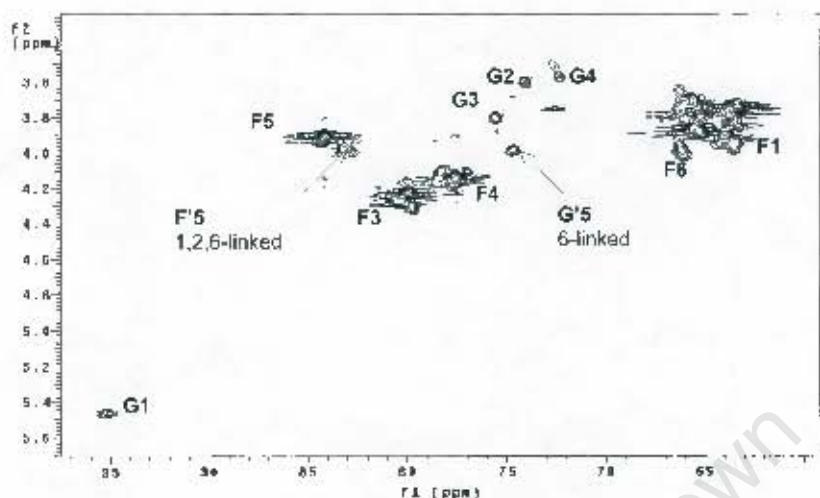


Figure 4.20: The HSQC spectrum of the *Agave americana* water extract

The signals from 106.10 to 106.92 ppm correspond to the anomeric region (C2) of β -D-Fruf residues. The *Agave americana* inulin spectrum contains several peaks in this region indicating that C2 exists in many different environments. The most intense peak in this region, at 106.64 ppm, was assigned to C2 of the internal (2 \rightarrow 1) β -D-Fruf units.

Methylation analysis provides evidence for branching of the fructosyl chain and this is confirmed by the NMR data. The signal at 84.20 ppm was assigned to C5 of the internal units of the fructan. The small peak upfield at 83.18 ppm was assigned to C'5 of the 1,2,6-linked β -D-Fruf, for which the glycosylation of C6 results in a shielding of C5 (γ effect). This key assignment provides further evidence to support branching of the saccharide. Therefore the resonances in the anomeric region, at 106.10 and 106.20 ppm, are assigned to C2 of those residues involved in branching (i.e. 1,2,6-linked β -D-Fruf units) and C2 of those terminal residues linked to the polymer backbone as well as the terminal fructose.

Many overlapping signals occur for C1 and C6 of β -D-Fruf, in the regions of 63.28 to 63.73 ppm and 65.28 to 66.30 ppm respectively. These peaks were assigned based on comparison of chemical shifts with literature values.²²⁻⁴⁴ The overlapping signals at this chemical shift are due to the different fructosyl residues present namely, the most abundant (2 \rightarrow 1) linked internal units, the branch point residues (1,6 \rightarrow 2 linked) and the

terminally 2-linked residues. The peak at 77.55 ppm is attributed to C4 of β -D-Fruf and the peak at 80.00 ppm to C5 of β -D-Fruf.

The low intensity signals were assigned to glucose with the anomeric glucose carbon appearing at a chemical shift of 95.17 ppm and the other ring carbons appearing in the region of 72.70 to 69.42 ppm. Use of proton-proton correlation experiments (data not shown) and closer inspection of the HSQC (Figure 4.20) spectrum indicated the presence of two glucose spin systems. The first corresponding to terminal non-reducing glucose (1-linked), as found for the chicory inulin and the second to the internal glucose [(1 \rightarrow 6) linked]. Evidence for the presence of β -D-Fruf linked to C6 of glucose followed from the upfield shift of the C5 carbon resonance shown in Figure 4.20.

4.5 Conclusion

This project aimed at characterising the composition and structure of the fructose rich saccharides in the water extract of *Agave americana*. The three factors considered were the monosaccharide composition, the molecular size and the glycosidic linkages between the residues.

HPAEC-PAD confirmed the composition of the saccharides to be a fructan, composed of glucose and fructose. SEC showed the polymers to be ≥ 1800 Da with a DP ≥ 10 . Size analysis by HPAEC-PAD suggested that the saccharides have a DP range of 16 to 20 and the average DP estimated by ^1H NMR was found to be 16. Complementary results of methylation analysis and NMR spectroscopy (one and two dimensional) suggests that the structure of *Agave americana* is a polymer made up of a back bone of (2 \rightarrow 1) linked β -D-Fruf residues, with a terminal (1-linked) or an internal (1 \rightarrow 6 linked) glucosyl residue and that approximately every third fructosyl residue in the polymer backbone is branched through C6.

Inulin has been isolated from many sources in the botanical world. The structure of inulin is commonly a terminal glucose followed by a chain of fructose residues however; there exists diverse variation in structure as reported in literature and listed below.

In many plants of the *Compositae* genus, e.g. *Cichorium intybus* (chicory root), linear inulin type fructans [β -(2 \rightarrow 1) linked] are abundant. In another species of the *Compositae* family, *Matricaria maritima*, the main water-soluble carbohydrate component was found to be a linear chain of β -(2 \rightarrow 1) linked fructose units with a terminal glucose.²³ In wheat and rye, graminans (levan and inulin type mixed fructans) have been found.²⁵

In the *Avena* and *Lolium* genus, internally linked and terminal glucose residues exist. Within the *Lolium* genus, linear and branched fructans with primarily β -(2 \rightarrow 6) linked fructose units were found. In other species, e.g. *Triticum aestivum*, branched fructans have been discovered where a fructose residue is linked to three other residues.⁵⁰

Fructans occur as storage polymers in the *Echinacea* species as well. In *Echinacea purpurea*, fructans are present predominantly as linear β -(2 \rightarrow 1) linked fructans with

exclusively terminal glucose residues. A small fraction of 1,2,6 linked β -D-Fruf units (branch points) were detected.²⁴

There has also been great structural diversity found within the agave species. The main storage carbohydrate in *Agave tequilana* was found to be an inulin type fructan with β -(2 \rightarrow 1) linkages between the residues. Investigation of *Agave vera cruz* revealed the presence of a complex mix of branched fructans containing β -(2 \rightarrow 1) linked and β -(2 \rightarrow 6) linked residues. Internal glucoses were also found. Reports on *Agave deserti* showed that the predominant FOS was a fructan of DP 3 containing an internal glucose residue.¹⁹

The compositional and structural results presented here suggest that *Agave americana* produces a fructan that is similar to that reported for *Agave vera cruz* and that it could be a potential source of commercial inulin suitable for use as a prebiotic.

5 Conclusion

In this project, composition and structural studies were carried out on water-soluble extracts isolated from local species of aloe (*Aloe ferox*) and agave (*Agave americana*) in light of them being possible sources of commercial health products.

This study specifically focussed on the non-pectic water-soluble saccharides found in the leaves of *Aloe ferox*, in an attempt to compare chemical structure with the commercially produced immunomodulatory molecule, acemannan, derived from *Aloe vera*.

SEC analysis revealed that a range of polymer sizes were present in the water-soluble extract of the *Aloe ferox* parenchyma with a large percentage of low-molecular material, comprising of pectic polymers. Monosaccharide analysis found that the saccharides were composed mainly of glucose, galactose and mannose; and from these experiments it was noted that the overall percentage of total sugar assayed was very low, between 10-25 %. These results differed from the literature results of *Aloe vera* which showed that the polymers present in *Aloe vera* are highly water-soluble and rich in mannose.

An alternative method of extraction (by ultrasound treatment) was tested in order to increase the amount of carbohydrate released. Ultrasonic waves did release a greater amount of water-soluble material, however not sufficiently high relative to *Aloe vera*. A comparative study of *Aloe ferox* leaves from different sources showed that environmental conditions affect the monosaccharide composition of leaves, hence the difference in results compared to literature reports.

The overall conclusion from this study is that the polysaccharides in *Aloe ferox* leaves are not highly water-soluble. No glucomannan similar to acemannan could be detected as mannose and glucose, although present, were found in very low amounts and occurred in a ratio of 3:2 instead of the expected 15:1. Therefore *Aloe ferox* cannot be considered as a direct substitute for *Aloe vera*, but has certain characteristics that may make its use of value in industry.

The analysis of the water-soluble saccharides present in the heart of *Agave americana* gave more promising results. HPAEC-PAD confirmed the composition of the saccharides to be a fructan, composed of glucose and fructose. SEC showed the polymers to be ≥ 1800 Da with a DP ≥ 10 . Size analysis by HPAEC-PAD suggested that the saccharides have a DP range of 16 to 20. The average DP estimated by ^1H NMR was found to be 16.

Linkage studies by methylation analysis (by GC-MS) and structural studies by NMR spectroscopy found that the structure of the saccharides in *Agave americana* to be a polymer made up of a back bone of (2 \rightarrow 1) linked β -D-Fruf residues, with a terminal (1-linked) or an internal (1 \rightarrow 6 linked) glucosyl residue, and that approximately every third fructosyl residue in the polymer backbone is branched through C6. Two dimensional NMR was used to confirm the overall structure. The compositional and structural results presented here suggest that *Agave americana* produces a fructan that is similar to that reported for *Agave vera cruz* and that it could be a potential source of commercial inulin suitable for use as a prebiotic.

Further work on this project would entail full confirmation of the structure by use of enzymatic specific cleavages of the fructan and detailed analysis of the derived oligosaccharide fragments.

6 References

1. G. O. Aspinall (ed.), in *The Polysaccharides*, Academic Press, New York, 1983, vol. 1, pp. 1-18.
2. A. Chesson, in *Food Polysaccharides and their Applications*, ed. A. M. Stephen, Marcel Dekker, 1995, pp. 547-576.
3. A. G. J. Voragen, W. Pilnik, J. F. Thibault, M. A. V. Axelos and C. M. G. C. Renard, in *Food Polysaccharides and their Applications*, ed. A. M. Stephen, Marcel Dekker, 1995, pp. 287-340.
4. J. T. Chow, D. A. Williamson, K. M. Yates and W. J. Goux, Chemical characterisation of the immunomodulating polysaccharide of *Aloe vera* L., *Carbohydrate Research*, 2005, **340**, 1131-1142.
5. K. R. Niness, Inulin and oligofructose: What are they?, *Journal of Nutrition*, 1999, **129**, 1402-1406.
6. <http://www.plantzafrica.com/plantab/aloeferox.htm> (06/02/2005)
7. K. Eshun, Q and He, *Aloe vera*: A valuable ingredient for the food, pharmaceutical and cosmetic industries – a review, *Critical Reviews in Food Science and Nutrition*, 2004, **44**, 91-96.
8. www.theinstitute.ch/images/Aloe_ferox1.jpg (28/09/2005)
9. A. Femenia, P. Garcia-Pascual, S. Simal and C. Rosello, Effects of heat treatment and dehydration on bioactive polysaccharide acemannan and cell wall polymers from *Aloe barbadensis* Miller, *Carbohydrate Polymers*, 2003, **51**, 397-405.

10. A. Femenia, E. S. Sanchez, S. Simal and C. Rosello, Compositional features of polysaccharides from *Aloe vera* (*Aloe barbadensis* Miller) plant tissues, *Carbohydrate Polymers*, 1999, **39**, 109-117.
11. www.healthbells.co.za (08/06/2005)
12. <http://www.vegetaryen.net/beslenme/urunler/images/aloe-vera.jpg> (05/02/2007)
13. I. Sun-A, O. Sun-Tack, S. Sukgil, K. Mi-Ran, K. Dong-Seon, W. Sung-Sick, H. J. Tae, I. P. Young and L. Chong-kil, Identification of optimal molecular size of modified *Aloe* polysaccharides with maximal immunomodulatory activity, *International Immunopharmacology*, 2005, **5**, 271-279.
14. Y. Ni, D. Turner, K. M. Yates and I. Tizard, Isolation and characterisation of structural components of *Aloe vera* L. leaf pulp, *International Immunopharmacology*, 2004, **4**, 1745-1755.
15. X. L. Chang, C. Wang, Y. Feng and Z. Lui, Effects of heat treatments on the stabilities of polysaccharides substances and barbaloin in gel juice from *Aloe vera* Miller, *Journal of Food Engineering*, 2006, **75**, 245-251.
16. http://tucsoncactus.org/plants_db_images/Aloe.ferox.KB.jpg (05/02/2007)
17. E. Dagne, D. Bisrat, A. Viljoen and B. E. van Wyk, Chemistry of *Aloe* species, *Current Organic Chemistry*, 2000, **4**, 1055-1078.
18. www.alcare.co.za/aboutaloe.htm (05/02/2007)
19. M. G. Lopez, N. A. Mancilla-Margalli and G. Mendoza-Diaz, Molecular structures of fructans from *Agave tequilana* Weber var. azul, *Journal of Agricultural and Food Chemistry*, 2003, **51**, 7835-7840.
20. G. Iniguez-Covarrubias, R. Diaz-Teres, R. Sanjuan-Duenas, J. Anzaldo-Hernandez and R. M. Rowell, Utilisation of by-products from the tequila industry.

Part 2: potential value of *Agave tequilana* Weber azul leaves, *Bioresource Technology*, 2001, **77**, 101-108.

21. A. Van Laere and W. Van Den Ende, Inulin metabolism in dicots: chicory as a model system, *Plant, Cell and Environment*, 2002, **25**, 803-813.
22. X. Chen and G. Tian, Structural elucidation and antitumor activity of a fructan from *Cyathula officinalis* Kuan, *Carbohydrate Research*, 2003, **338**, 1235-1241.
23. S. Cerantola, N. Kervarec, R. Pichon, C. Magne, M. Bessieres and E. Deslandes, NMR characterisation of inulin-type fructooligosaccharides as the major water-soluble carbohydrates from *Matricaria maritima*, *Carbohydrate Research*, 2004, **339**, 2445-2449.
24. M. Wack and W. Blaschek, Determination of the structure and degree of polymerisation of fructans from *Echinacea purpurea* roots, *Carbohydrate Research*, 2006, **341**, 1147-1153.
25. P. Strober, S. Benet and C. Hischenhuber, Simplified enzymatic high-performance anion-exchange chromatographic determination of total fructans in food and pet food – Limitations and measurement uncertainty, *Journal of Agricultural and Food Chemistry*, 2004, **52**, 2137-2146.
26. T. S. Manning and G. R. Gibson, Prebiotics, *Best Practice and Research Clinical Gastroenterology*, 2003, **18** (2), 287-298.
27. G. Iniguez-Covarrubias, S. E. Lange and R. M. Rowell, Utilisation of by-products from the tequila industry. Part 1: Agave bagasse as a raw material for animal feeding and fibreboard production, *Bioresource Technology*, 2001, **77**, 25-32.
28. <http://www.botanical-online.com/floragaveamericana.jpg> (22/01/2007)
29. P. Harris, A. Morrison and C. Dacombe, in *Food Polysaccharides and their Applications*, ed. A. M. Stephen, Marcel Dekker, 1995, pp. 577-606.

30. M. F. Chaplin (ed.), *Carbohydrate Analysis – A Practical Approach Second Edition*, Oxford University Press, 1994, pp. 7-8.
31. N. C. Carpita and E. M. Shea, in *Analysis of Carbohydrates by GLC and MS*, ed. C. J. Biermann and G. D. McGinnis, CRC Press, Boca Raton, 1989, pp. 157-216.
- 31a. www.epa.gov/superfund/programs/dfa/download/meth_gcm.pdf (25/05/2007)
32. H. Bjorndal, C. G. Hellerqvist, B. Lindberg and S. Svensson, Gas-liquid chromatography of mass spectrometry in methylation analysis of polysaccharides, *Angew Chem*, 1970, **82**, 610-619.
33. A. Dell, A. J. Reason, K. H. Khoo, M. Panico, R. A. McDowell and H. R. Morris, Mass spectrometry of carbohydrate-containing biopolymers, *Methods in Enzymology*, 1994, **230**, 86-108.
34. J. D. Timpa, Application of universal calibration in gel permeation chromatography for molecular weight determination of plant cell wall polymers: Cotton Fibre, *Journal of Agriculture and Food Chemistry*, 1991, **39**, 270-275.
35. S.C. Churms, Recent progress in carbohydrate separation by high-performance liquid chromatography based of size exclusion, *Journal of Chromatography A*, 1996, **720**, 151-166.
36. G. D. Christian, *Analytical Chemistry*, Wiley, 5th edn., 1994.
37. D. A. Skoog, D. M. West and F. J. Holler, *Fundamentals of Analytical Chemistry*, Saunders College Publishing, 7th edn., 1997.
38. <http://www.cem.msu.edu/~reusch/VirtualText/Spectrpy/MassSpec/masspec1.htm> (18/09/2006)

- 38a. <http://masspec.scripps.edu/publications/public.php> (24/05/2007)
39. A. J. Mort and M. L. Pierce, in *Journal of Chromatography*, ed. Z. E. Rassi, Elsevier Science, 2002, **66**, 207-250.
40. Gradient elution in ion chromatography: anion-exchange with conductivity detection, *Dionex*, 1987, TN 19.
41. P. M. Collins and R. J. Ferrier, *Monosaccharides Their chemistry and their roles in natural products*, Wiley, 1995, pp. 463-524.
42. A. S. Perlin and B. Casu, *The Polysaccharides*, ed. G. O. Aspinall, Academic Press, New York, 1983, vol. 1, pp. 133-193.
43. D. H. Williams and I. Fleming, *Spectroscopic Methods in Organic Chemistry*, McGraw-Hill, London, 5th edn., 1995.
44. H. C. Jarrell, T. F. Conway and P. Moyna, I. C. P. Smith, Manifestation of anomeric form, ring structure, and linkage in the ¹³C-N.M.R spectra of oligomers and polymers containing D-fructose: maltulose, isomaltulose, sucrose, leucrose, 1-kestose, nystose, inulin, and grass levan, *Carbohydrate Research*, 1979, **76**, 45-57.
45. W. Mabusela, A. M. Stephen and M. C. Botha, Carbohydrate polymers from *Aloe ferox* leaves, *Phytochemistry*, 1990, **29**, 3555-3558.
46. M. C. Botha, Process for extracting polysaccharides from plant material, *South African Patent*, 1994, 94/1581.
47. Z. Hromadkova and A. Ebringerova, Ultrasonic extraction of plant materials – investigation of hemicellulose released from buckwheat hulls, *Ultrasonics Sonochemistry*, 2003, **10**, 127-133.

48. J. X. Sun, R. C. Sun, X. F. Sun and Y. Q. Su, Fractional and physico-chemical characterization of hemicelluloses from ultrasonic irradiated sugarcane bagasse, *Carbohydrate Research*, 2003, **339**, 291-300.
49. S. Farine, C. Versluis, P. J. Bonnici, A. Heck, J. L. Peschet, A. Puigserver and A. Biagini, Separation and identification of enzymatic sucrose hydrolysis products by high-performance anion-exchange chromatography with pulsed amperometric detection, *Journal of Chromatography A*, 2001, **920**, 299-308.
50. N. Pavis, N. J. Chatterton, P. A. Harrison, S. Baumgartner, W. Praznik, J. Boucaud and M. P. Prud'homme, Structure of fructans in roots and leaf tissues of *Lolium perenne*, *New Phytologist*, 2001, **150**, 83-95.

APPENDIX 1

1.1 Phenol-sulphuric acid assay

1. A portion (0.5 mL) of solution containing the carbohydrate is placed into a boiling tube.
2. Distilled water (0.5 mL) is added, followed by 80 % phenol (25 μ L).
3. Concentrated H_2SO_4 (2.5 mL) is rapidly added onto the liquid surface of the mixture.
4. The tubes are shaken and then allowed to stand for 10 – 20 min to allow the temperature to fall to $\sim 25^\circ\text{C}$.
5. The absorbance was measured at 490 nm against a blank.
6. The carbohydrate content is read off a calibration graph of absorbance vs. glucose concentration.

1.2 Carbazole assay

Reagents

- A Dissolve sodium tetraborate decahydrate (0.9 mg) in water (10 mL) and add ice-cold 98 % concentrated H_2SO_4 (90 mL) carefully to form a layer. Leave undisturbed overnight to mix without excessive heat production. Check to see if thoroughly mixed and at RT before use.
- B Dissolve carbazole – recrystallised from ethanol, (100 mg) in of absolute ethanol (100 mL).

Method

1. Cool the samples, standards and controls (0.5 mL) in an ice-bath.
2. Carefully add ice-cold reagent A (3 mL) with mixing and cooling in an ice-bath.
3. Heat the mixtures at 100 °C for 10 min.
4. Cool rapidly in an ice-bath.
5. Add reagent B (100 μl) and mix well.
6. Re-heat at 100 °C for 15 min.
7. Cool rapidly to RT and measure absorbance at 525 nm.

1.3 GC and HPAEC sample preparation

Step 1: Hydrolysis

1. The sample (10 mg) is hydrolysed with 2M TFA (2 mL) at 125 °C for 1 h.
2. The extract is allowed to cool down and is then transferred to a round bottom flask.
3. Methanol is added and the content was concentrated under reduced pressure on a rotary evaporator at 40 °C to remove excess TFA as an ester.

Step 2: Reduction

1. Add 1 mL of distilled water and add a spatula tip full of NaBH_4 and leave at RT for at least 1 h.
2. Check that the pH is basic before proceeding further, if not then add more NaBH_4 .
3. Add acetic acid dropwise until effervescence stops.
4. Add methanol/acetic acid solution (2 mL, 1:1) and concentrate under reduced pressure on a rotary evaporator at 40 °C.
5. Repeat this step 4 times.
6. Then add methanol only and concentrate under reduced pressure on a rotary evaporator at 40 °C, to remove the borate and the methyl esters.

Step 3: Acetylation

1. Add pyridine (0.4 mL) and acetic anhydride (1 mL) and reflux for 1 hr at 100 °C.
2. Allow to cool then concentrate under reduced pressure on a rotary evaporator at 40 °C to remove any solvent.
3. Wash the contents with CHCl_3 (5 mL) and transfer to a glass centrifuge tube.
4. Add millipore water, vortex and then centrifuge gently.
5. After centrifugation, remove the top aqueous layer using a Pasteur pipette.
6. Repeat the vortex and centrifuge step with acidified water, water, water with bicarbonate and finally water again.
7. Filter the CHCl_3 layer through Na_2SO_4 and a piece of cotton wool using a Pasteur pipette.
8. The sample is now ready for injection into the GC.

1.4 Permethylation using NaOH and MeI

1. Dry the sample to be methylated in a glass tube with a Teflon-lined screw cap.
2. Place 5 pellets of NaOH in a dry mortar, crush into a powder and then add of dry DMSO (~ 3 mL) using a Pasteur pipette. This step should be done as quickly as possible to minimize absorption of moisture from the atmosphere.
3. Take up 0.5 to 1 mL of the DMSO-NaOH slurry with a Pasteur pipette and add to the sample.
4. Add methyl iodide (about 0.5 mL) and mix vigorously. Place the reaction mixture on an automatic shaker for 10 min at RT.
5. Quench the reaction by careful, dropwise addition of water (about 1 mL) with constant shaking between additions to lessen the effects of the highly exothermic reaction.
6. Add chloroform (2 mL), mix thoroughly, and allow the mixture to settle into two layers. Centrifuge the mixture to assist better separation if necessary.
7. Remove and discard the upper aqueous layer and wash the lower chloroform layer several times with water, until the water being removed is completely clear.
8. Filter the chloroform layer through Na_2SO_4 .
9. Dry the chloroform layer under a stream of nitrogen and dissolve the residue in methanol for analysis.